NASA TECHNICAL NOTE

NASA TN D-5813

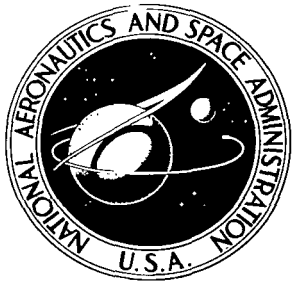

NASA TN D-5813

CONDENSERS AND BOILERS FOR STEAM-POWERED CARS: A PARAMETRIC ANALYSIS OF THEIR SIZE, WEIGHT, AND REQUIRED FAN POWER

by William C. Strack

Lewis Research Center
Cleveland, Ohio 44135

NATIONAL AERONAUTICS AND SPACE ADMINISTRATION • WASHINGTON, D. C. • MAY 1970

1. Report No. NASA TN D-5813	2. Government Accession No.
3. Recipient's Catalog No.	
4. Title and Subtitle CONDENSERS AND BOILERS FOR STEAM-POWERED CARS: A PARAMETRIC ANALYSIS OF THEIR SIZE, WEIGHT, AND REQUIRED FAN POWER	5. Report Date May 1970
	6. Performing Organization Code
7. Author(s) William C. Strack	8. Performing Organization Report No. E-5275
9. Performing Organization Name and Address Lewis Research Center National Aeronautics and Space Administration Cleveland, Ohio 44135	10. Work Unit No. 126-15
	11. Contract or Grant No.
	13. Type of Report and Period Covered Technical Note
12. Sponsoring Agency Name and Address National Aeronautics and Space Administration Washington, D.C. 20546	14. Sponsoring Agency Code

15. Supplementary Notes

16. Abstract

Size, weight, and performance of conventional condensers and boilers for steam-powered cars are analytically investigated. Fan power is presented over a range of design and operating variables such as heat-exchanger size, heating rate, and ambient air temperature. It is found that practical condensers are about four or five times the size of conventional automobile radiators. Boiler size is not necessarily large - 100-lb (45-kg) boilers are possible for 4000-lb (1815-kg) passenger cars. The weight and fuel economy of a complete propulsion system are estimated to be quite comparable to today's internal-combustion systems.

17. Key Words (Suggested by Author(s)) Automobile, Boilers, Steam, Heat exchangers, Condensers	18. Distribution Statement Unclassified - unlimited

19. Security Classif. (of this report)	20. Security Classif. (of this page)	21. No. of Pages	22. Price*
Unclassified	Unclassified	64	$3.00

*For sale by the Clearinghouse for Federal Scientific and Technical Information Springfield, Virginia 22151

CONTENTS

CONDENSERS AND BOILERS FOR STEAM-POWERED CARS: A PARAMETRIC ANALYSIS OF THEIR SIZE, WEIGHT, AND REQUIRED FAN POWER

by William C. Strack

Lewis Research Center

SUMMARY

An analytic examination of conventional condensers and boilers for a hypothetical 4000-pound (1815-kg) steam-powered passenger car is made to determine their size, weight, and required fan power. A single fin-and-tube condenser configuration is examined over a range of frontal area, depth, heat-transfer rate, ambient air temperature, and condensation temperature. The boiler is assumed to be a once-through helix configuration. Variations in the tube diameter, tube spacing, boiler diameter, and combustion gas inlet and exit temperatures are considered. For both heat exchangers, emphasis is focused on the tradeoff between exchanger size and fan power requirements. A total propulsion system model is employed to study the interaction between the thermodynamic parameters and the heat-exchanger parameters. The model is for a hypothetical 4000-pound (1815-kg) passenger car with 175 shaft horsepower (130 kW). The performance of this car (e.g., acceleration and top speed) is comparable to today's typical passenger car of the same weight.

Condenser fan power is found to be quite low (under 1 hp (0.7 kW)) at most operating conditions. However, condenser fan power requirements are very large (over 50 hp (37 kW)) under peak-power or hot-day conditions unless the condenser is four or five times larger than a conventional automobile radiator or the condensation temperature is temporarily increased at such times. Boiler weight could be of the order of 100 pounds (45 kg) and the volume about 1.6 cubic feet (0.045 m^3), not including the burner, blower, and control assemblies.

The total steam propulsion system could be designed to weigh approximately the same as a conventional automobile propulsion system. The overall fuel cost would be no greater, and perhaps less, than today's average car.

INTRODUCTION

The analytic study reported herein examined the size, weight, and performance of the two heat exchangers required in steam cars. Both the condenser and the steam generator have often been the target of steam-car criticism because of their historically large size and weight. Typical existing automotive steam-generating units for 60- to 150-shaft-horsepower (45- to 112-kW) powerplants occupy 4 to 6 cubic feet (0.113 to 0.17 m^3) and weigh 225 to 325 pounds (102 to 148 kg) including the blower and fan motor (refs. 1 to 5). Typical condensers range from common automotive radiators weighing about 30 pounds (14 kg) to larger units weighing 140 pounds (63 kg) including fan and housing. Beyond this, very little published information is available concerning the performance of these heat exchangers. It is important to know, for instance, if the smaller condensers have sufficient capacity to handle peak-power and hot-day situations without venting steam or demanding an extreme amount of fan power. Venting steam is undesirable since it necessitates more frequent refills and because it could produce a visibility hazard to following vehicles. Since fan power reduces the useful power and requires a motor or drive mechanism, it is important to avoid high values of air-side pressure drop. It is also important to know if the size and weight of these heat exchangers can be reduced by careful selection of such factors as geometry, tubing sizes, and design temperatures.

The answers to these questions are sought herein. No attempt is made to determine an optimum heat-exchanger design in terms of some performance criterion. This would be artifical at this point as many of the influencing factors are presently unknown. For example, the tradeoff of exchanger size against fan power depends on the cost and complexity of the fan drive mechanism as well as on overall efficiency. Nevertheless, it is clear that the design goals would include making the exchangers as small and lightweight as possible without incurring a "large" fan power requirement. Therefore, exchanger size and fan power are used as joint performance criteria.

Since some of the ways of improving the performance have an adverse affect on the fuel economy, the analysis must consider this interaction also. To do this, a simple propulsion system model is formed for a typical 4000-pound (1815-kg) passenger automobile with a maximum shaft power of 175 horsepower (130 kW). Due to differences in parasitic losses, this power rating is equivalent to an internal-combustion (IC) engine rated at about 290 horsepower (220 kW). The performance of these two powerplants is quite comparable; they each provide a top speed of about 110 miles per hour (177 km/hr) and acceleration from 0 to 60 miles per hour (0 to 97 km/hr) in about 10 seconds. Reference 1 discusses these parasitic losses and performance comparisons in more detail. The model provides a framework for the tradeoff between the heat-transfer performance

and the thermodynamic performance. It also allows a fuel consumption comparison between steam cars and existing IC-powered cars.

NASA is not charged with responsibility for motor vehicle research. However, in view of the Agency's related expertise developed in connection with power generating equipment for spacecraft, the preparation of the present report seemed like an appropriate contribution to the present campaign against pollution. The recent interest in steam-powered vehicles is due to their very low level of air-pollution emissions together with several other attractive features. This situation is reviewed in the next section to provide some background information for those readers unfamiliar with it. It may be skipped without loss of continuity.

POLLUTION BACKGROUND

A great deal of attention today is focused on methods to reduce air pollution. This attention stems from the fact that our cities are already inflicted with uncomfortable, annoying, and often harmful amounts of pollutants (refs. 6 and 7). Air pollution is responsible for crop losses, property damage, frequent cleaning costs, chronic respiratory diseases, and perhaps adverse weather modification.

The common internal-combustion engine used in land vehicles is a major source of these pollutants. This is illustrated in figure 1 (from ref. 7), where the amount of individual contaminants from automobiles is compared to all other sources. About 60 percent of all U.S. air pollution comes from motor vehicles (ref. 7). Hence, the IC engine has been the target of much controversy in regard to both its potential improvement and its possible replacement. While some significant reductions in the exhaust emissions of IC engines have recently been achieved, substantial further decreases will be very difficult to attain. Indeed, it seems rather improbable that acceptable pollution levels can ever be attained without a great deal of mechanical complexity and cost penalties. This matter is serious enough to have caused interest in alternative propulsion systems.

There are of course a multitude of other factors besides air pollution that must be considered in the search for a satisfactory substitute for the IC engine. These factors are discussed at length in references 1 to 4 and 7 to 10. The next several paragraphs briefly review prospective alternative systems.

Fuel-cell systems are limited by low specific power. This means that they would only be able to travel at limited maximum speeds, and would be unable to accelerate or climb grades at reasonable rates. Such power-limited vehicles would be a hazard on high-speed roads and likely increase traffic congestion in urban areas.

Battery systems do not look attractive for reasons dependent on the type of battery. The organic electrolyte batteries are power limited just as the fuel cells. Lead-acid,

nickel-cadmium, and nickel-zinc batteries, however, are energy limited. This means that their energy density is so low that it severely limits the vehicle's range before recharging (or exchanging). Some unconventional types such as silver-zinc, sodium-sulfur, and lithium-chlorine batteries do not suffer from either low specific power or low specific energy. But they are either very expensive, hazardous, or both, and most are quite experimental at present. Also, the world supply of many battery materials such as copper, lead, tin, and zinc is rather limited. A complete changeover to battery-powered vehicles might put severe strains on both the price and supply of some of these materials.

The gas turbine engine has very favorable specific power and energy characteristics. And, like fuel cell and battery systems, it is a low pollution device. However, a combination of high off-design fuel consumption, sluggishness of throttle response, problems in power transmission, and high manufacturing cost in small sizes reduces the attractiveness of the gas turbine for automobile application.

External-combustion (EC) engines have received much recent attention because of their very low pollution characteristics. One of these, known as the Stirling engine (refs. 11 and 12), was developed for military purposes. Besides its very low pollution level, the Stirling engine is very quiet and has multifuel capability and high efficiency. Unfortunately, it is also rather heavy, costly, and slow in regard to response time to a change in load.

The Rankine-cycle reciprocating steam engine is also an EC device. It is somewhat less polluting than either the gas turbine or the Stirling engine, quiet, and not too complex. It has multifuel capability, high specific power and energy, moderate efficiency, and a very favorable torque-against-speed curve. The latter characteristic is very important in that it minimizes or even eliminates a transmission requirement. Its total system weight and mass production cost appear to be comparable to today's IC systems, although this has not as yet been proven. Among its disadvantages are (1) the working fluid freezes in cold weather, (2) lubrication problems at high temperatures, and (3) bulkiness. Nonetheless, after all factors are considered, many investigators conclude that the reciprocating steam engine is at least a reasonable alternative to IC engines for automotive applications (refs. 1 to 3, 8, and 10).

Rankine cycles employing a steam turbine instead of a reciprocating expander would be relatively simple and lightweight. However, steam turbines for automobiles would be very small and relatively inefficient. Furthermore, they would involve high rotational speeds and require speed reduction gearing. These disadvantages are presently thought to outweigh its advantages relative to a reciprocating expander. Rankine-cycle engines employing working fluids other than water have some interesting advantages. They would eliminate the water freezing problem and could also alleviate lubrication problems. However, the usual organic fluids considered, such as Freon-11 and

Dowtherm-A, become unstable at temperatures above approximately 300° to 700° F (420 to 650 K). Moreover, their combination of both chemical and thermodynamic properties leads to a less efficient thermodynamic cycle. It is presently unclear as to which fluid is best in an overall sense, but water is certainly a prime contender.

In figure 2 existing steam engines are compared with emission-controlled IC engines - both existing and future - with respect to air pollution. The data were compiled from references 1 and 7. The individual contaminants are shown on a mass basis relative to present uncontrolled automobile engines. Present IC engines with emission controls reduce carbon monoxide emissions by a factor of 3. The expected ultimate reduction factor (after 1980) is about 15. But existing steam engines without controls already achieve reduction factors on the order of 1000. The hydrocarbon emission comparison is roughly the same. The nitrogen oxides comparison is less strong, showing reduction factors of 10 to 30 for the steam engine. The lead compound emissions drop to zero for steam engines since they burn unleaded (and cheaper) fuels. The important point is that present steam engines pollute far less than existing or predicted future engines and do so without any costly and complicated control devices. This is because the combustion process in the steam engine is continuous and at lower temperatures and pressures than the IC engine combustion process.

ANALYSIS

Thermodynamic Cycle

The simple steam Rankine cycle used to calculate the thermodynamics is illustrated in figure 3 by a schematic diagram and a temperature-entropy diagram (not to scale). Beginning at state 1, water is heated, evaporated, and superheated in the steam generator (boiler) until state 2 is reached. The superheated steam is then expanded to state 3 in an engine that produces work. The steam is then condensed to state 4 where it enters a pump that returns it to state 1.

Ideally, no pressure drops occur in the boiler and the condenser. Also, an ideal pump would raise the pressure of the saturated liquid isentropically from state 4 to 1. The deviations from these ideals can be important from a structural viewpoint since it means that the actual maximum system pressure may be quite a bit higher than the ideal maximum pressure. This, in turn, must be reflected in the pump design and the boiler tubing wall thickness. Also, an ideal expansion process would be isentropic and terminate at state 3' instead of 3. The deviation from this ideal is very important thermodynamically since the useful work produced by the engine is strongly affected by such a deviation.

The main concern with cycle analysis is the energy conversion efficiency of the device. This is called thermal efficiency and is defined as

$$\eta_{th} = \frac{\text{Work of engine - Pump work}}{\text{Heat added}} = \frac{(H_2 - H_3) - (H_1 - H_4)}{H_2 - H_1} \tag{1}$$

(All symbols are defined in appendix A.) In this study the assumed known variables are the boiler outlet temperature and pressure and the condensing steam temperature. This allows H_2, $H_{3'}$, and H_4 to be determined from steam tables (e.g., ref. 13). The engine work is determined by assuming an engine expansion efficiency η_e as follows:

$$H_2 - H_3 = (H_2 - H_{3'})\eta_e \tag{2}$$

The pump work is closely approximated by

$$H_1 - H_4 = \frac{v(p_1 - p_4)}{\eta_{pump}} \tag{3}$$

where η_{pump} is the pump efficiency and p_1 is taken to be the same as p_2. The heat added may be found by solving the last two equations for $H_2 - H_1$.

Propulsion System Model

The power balance of this cycle is

$$P_b + P_{pump} = P_e + P_c \tag{4}$$

and the thermal efficiency may be rewritten

$$\eta_{th} = \frac{P_e - P_{pump}}{P_b} \tag{5}$$

Only part of the engine power appears as useful shaft power since friction is present within the engine, the clutch, and the power shafting devices. The mechanical efficiency accounts for this:

$$P_{sh} = \eta_m P_e \tag{6}$$

The useful shaft power is applied to the wheels, the condenser fan, the boiler blower, the water pump, and the other accessories. Thus,

$$P_{sh} = P_{wh} + P_{fan} + P_{bl} + P_{pump} + P_{acc} \tag{7}$$

Eliminating P_{sh} and P_e by combining and rearranging the last three equations leads to the expression for the boiler power:

$$P_b = \frac{P_{wh} + P_{fan} + P_{bl} + P_{acc} + (1 - \eta_m)P_{pump}}{\eta_m \eta_{th}} \tag{8}$$

The water flow rate follows immediately:

$$\dot{m}_w = \frac{P_b}{H_2 - H_1} \tag{9}$$

The condenser power may then be calculated from

$$P_c = \dot{m}_w(H_3 - H_4) \tag{10}$$

To calculate overall powerplant efficiency it must be realized that not all the fuel energy expended in the boiler is used to heat water. Some is wasted in the boiler exhaust gases. The boiler efficiency η_b is the fraction of fuel energy transferred to the water and may be calculated with equation (B61) from appendix B.

The energy delivered to the boiler blower is recovered since it transfers this energy to the incoming air, and from the air it is transferred to the water in the boiler. Thus the total power delivered to the boiler water is

$$P_b = \eta_b P_{fuel} + P_{bl}$$

Hence,

$$P_{fuel} = \frac{P_b - P_{bl}}{\eta_b}$$

The overall powerplant efficiency is defined as the ratio of useful work to the fuel energy. Using this definition and the previous relation yields

$$\eta_{over} \equiv \frac{P_{wh}}{P_{fuel}} = \frac{P_{wh}\eta_b}{P_b - P_{bl}} \tag{11}$$

The rate of change of distance with volumetric fuel flow (i.e., the instantaneous gas mileage) is simply

$$\text{Instantaneous gas mileage} = \frac{\mathscr{V}}{\left(\frac{\dot{m}}{\rho}\right)_{fuel}} = \frac{\mathscr{V}}{\left(\frac{\rho h_{fuel}}{P}\right)_{fuel}} \tag{12}$$

The actual gas mileage experienced by a driver would be calculated by averaging this expression over an appropriate driving cycle.

The preceding set of equations describes the energy flow model. A block diagram summary of this model is shown in figure 4. This diagram shows where the original energy contained in the fuel is dissipated. Note that the energy supplied to the water pump and boiler blower is returned to the working fluid. The component assumptions are as follows:

(1) Mechanical efficiency, $\eta_m = 0.92$

(2) Engine expansion efficiency at rated power, $\eta_e = 0.70$

(3) Water pump efficiency, $\eta_{pump} = 0.50$

(4) Accessory power, $P_{acc} = 2$ hp (1.5 kW)

(5) Fuel density, $\rho_{fuel} = 50$ lb/ft^3 (800 kg/m^3)

(6) Fuel heating value, $h_{fuel} = 18\,500$ Btu/lb (43 000 kJ/kg)

The wheel power overcomes tire friction resistance, aerodynamic drag, gravity while climbing hills, and inertia while accelerating. The gravity force is

$$F_{grav} = W_{car} \sin\beta \approx W_{car} \tan\beta = W_{car}(\text{grade}) \tag{13}$$

where β is the angle between the road and horizontal, and its tangent is commonly referred to as "percent grade." The tire force is

$$F_{tire} = C_{fr} W_{car} \cos\beta \tag{14}$$

The aerodynamic resistance is given by

$$F_{aero} = \frac{1}{2}\rho v^2 C_D S \tag{15}$$

Finally, the wheel power for unaccelerated motion is given by

$$P_{wh} = (F_{tire} + F_{aero} + F_{grav})v = \left(C_{fr} W_{car} \cos\beta + \frac{1}{2}\rho v^2 C_D S + W_{car} \sin\beta\right)v \tag{16}$$

This relation is plotted in figure 5 for C_D and C_{fr} values based on reference 14 data and S = 24 square feet (2.23 m^2). Both car speed and grade have a strong influence on wheel power. At low speeds on a level road, tire friction predominates; but above 60 miles per hour (100 km/hr), air drag predominates as a cubic function of speed.

Condensers

A single condenser configuration was examined. This flat tube and ruffled fin design is shown in sketch a. A detailed description may be found in reference 15 under the

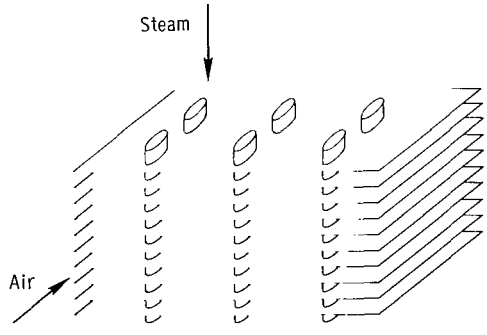

(a)

designation 11.32-737-SR. Since the steps involved in the heat-transfer calculations are conventional but tedious, the procedure is only touched upon here. The details are contained in appendix C.

Knowing the dimensions of a typical car makes it convenient to assume a condenser size and then proceed to calculate the fan power required under various operating conditions. By choosing the condenser frontal area and depth, the ambient air temperature,

the condensation temperature, and the steam flow rate, it is possible to iteratively solve for the air-side pressure drop. The fan power is easily calculated from the pressure drop and the fan efficiency (assumed to be 0.7).

The conventional log-mean rate equation is used for the heat-transfer rate. This is

$$q = UAF_G \Delta T_{lm} \tag{17}$$

where q is the overall heat-transfer rate, U is the overall thermal conductance, A is the heat-transfer area, F_G is a flow configuration correction factor equal to 1 for the cases of counterflow, boiling, or condensing, and ΔT_{lm} is the log-mean temperature difference of the air and water; U must be based on whichever area (air-side or water-side) A refers to.

The condenser is assumed to be constructed with copper fins and headers, and brass tubes. This is in accord with conventional radiator fabrication techniques. There is, however, a strong incentive to use aluminum in this application since weight and cost savings would be substantial. The weight equations are also given in appendix C.

Boilers

Only one boiler concept was examined. It consists of a single tube wound in a spiral to form concentric coils, and rows of these spirals stacked together like a stack of donuts. The shape of the boiler is thus a cylinder with a central void space as illustrated in sketch b. Employing monotube construction avoids complicated headers and has demonstrated safe operation. The water entering the boiler is heated to the saturation temperature in the liquid heating region. It is then vaporized in the boiling region, and the resulting steam is further heated in the superheat region. The combustion gas enters the end where the steam exits and therefore the boiler is a cross-counterflow arrangement. However, it can be accurately treated as a pure counterflow arrangement because there are many tube rows.

Sketch c illustrates the two fluid temperatures as a function of distance along the tube. Each of the three heat-transfer regions is treated separately insofar as the heat-transfer and fluid-friction calculations are concerned. The longitudinal and transverse tube spacing (see sketch d) is held fixed throughout the entire boiler, although the tube pitch ratios x_l and x_t are varied parametrically. The outside tube diameter is also held fixed throughout a single design. However, the tube inside diameter is a dependent variable. It is allowed to take on three different values depending on the maximum tube-wall temperature and water pressure in each of the three regions. This involves

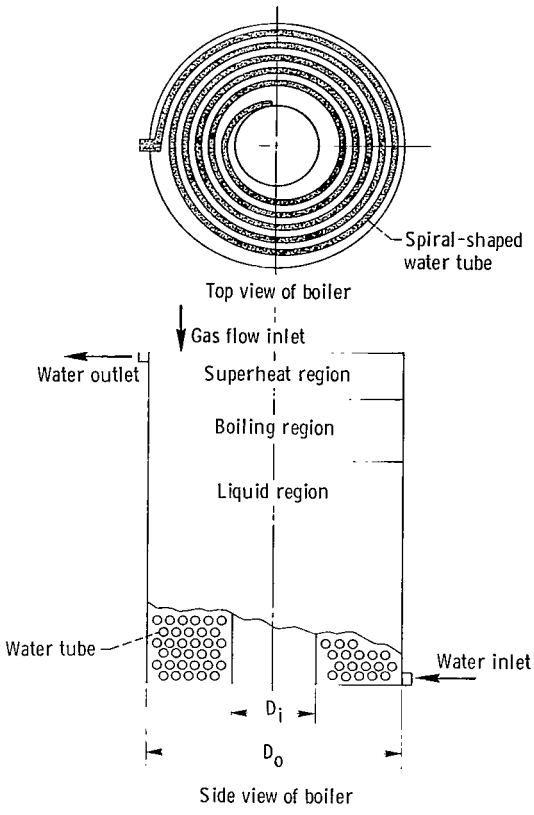
Spiral-shaped water tube
Top view of boiler
Gas flow inlet
Water outlet
Superheat region
Boiling region
Liquid region
Water tube
Water inlet
D_i
D_o
Side view of boiler

(b)

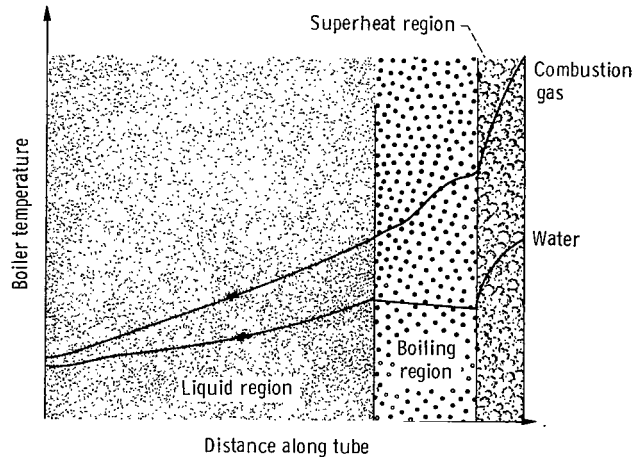
Superheat region
Combustion gas
Water
Boiling region
Liquid region
Boiler temperature
Distance along tube

(c)

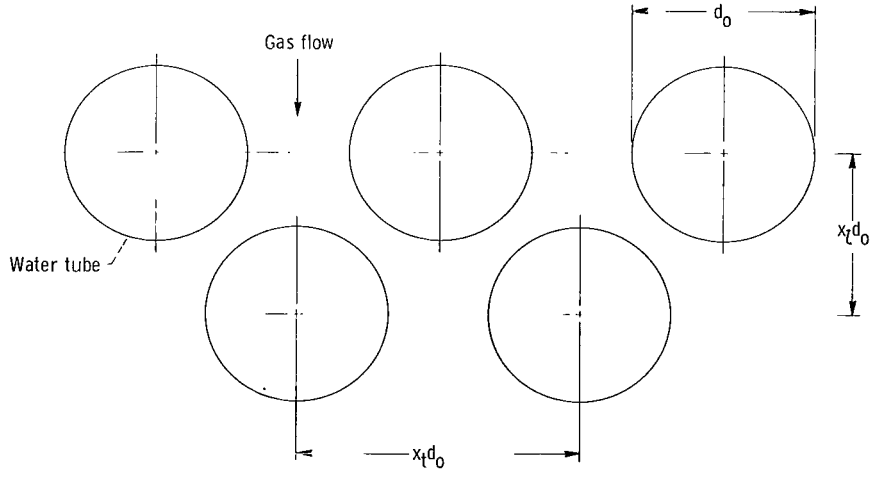
Gas flow
d_o
Water tube
$x_t d_o$
$x_t d_o$

(d)

an iteration on the water pressure at the inlet to each region. The superheat-region calculations are performed first, followed by the boiling-region calculations (using the superheat-region water inlet pressure as a first guess), and then the liquid-region calculations (using the boiling-region water inlet pressure as a first guess). By definition, the interface between the liquid and boiling regions is where the bulk water temperature is equal to the saturation temperature. Actually though, some subcooled boiling will occur in the liquid region because the tube-wall temperature is several degrees higher than the bulk water temperature near the interface. A sample calculation revealed that this effect is very small, however, and it was therefore ignored.

The details of the boiler calculations are set forth in appendix B. The tube material is a steel alloy known as modified 9M. It is composed of 9 percent chromium, 1 percent molybdenum, and very small amounts of columbium, vanadium, boron, nitrogen, and zirconium. This material costs about one-half as much as 316 stainless steel and yet has higher allowable stress up to 1050° F (840 K). It has already been used in SNAP-8 boilers (refs. 16 and 17) for the space program and its use for steam-car boilers appears to be an attractive application of that technology.

It should be pointed out that basically only one design configuration is being examined. There are many other configurations and concepts that might produce a better boiler. For example, finned tubing might reduce the boiler size and weight enough to offset its higher cost. Also, different flow arrangements might be more desirable. And it might be worthwhile to employ different materials, outside tube diameters, and tube spacings in the different heat-transfer regions. Variations such as these could be the subject for a more comprehensive analysis.

RESULTS AND DISCUSSION

Thermal Efficiency

The cycle calculations are summarized in figures 6 and 7 for a engine expansion efficiency of 0.7. Figure 6 shows that the thermal efficiency rises gradually with maximum cycle temperature (boiler outlet). Since expensive materials would have to be used at temperatures above approximately 1000° F (810 K), this value is picked for the baseline high temperature. Similarly, a boiler outlet pressure of 1500 psia (10.3 MN/m^2) is perhaps sufficiently high, although 2000 psia (13.8 MN/m^2) was arbitrarily selected as a baseline pressure for the boiler calculations. The thermal efficiency for a 2000 psia - 1000° F (13.8 MN/m^2 - 810 K) superheat cycle is 24 percent.

Although figure 6 indicates that a saturated cycle (i.e., without superheat) can yield thermal efficiencies up to about 21 percent, this is somewhat misleading since the curves

are drawn for constant engine expansion efficiency. In practice, the expansion efficiency for saturated cycles is significantly lower than for superheat cycles due to excessive condensation within the cylinders. If this effect were accounted for in figure 6, the curves would dip lower along and in the vicinity of the saturation line.

The curves in figure 6 are drawn for a condensation temperature of 212° F (373 K). The effect of condensation temperature on thermal efficiency is shown in figure 7. From an efficiency standpoint, very low temperatures are desirable. Below 212° F (373 K), the condensation pressure is subatmospheric and this would require either a vacuum system to remove leakage air or a hermetically sealed system. Furthermore, low condensation temperatures result in prohibitively large condensers. Thus, 212° F (373 K) is used as a baseline value. The baseline values of the three fundamental cycle variables are repeated here:

(1) Maximum steam temperature, 1000° F (810 K)

(2) Boiler outlet pressure, 2000 psia (13.8 MN/m^2)

(3) Condensation temperature, 212° F (373 K)

Condensers

The conventional automobile radiator dissipates about one-third to one-half of the waste heat load - the rest of it is in the exhaust gases. But the steam-car condenser handles nearly all the waste heat load. Thus, we can expect even a well-designed condenser to be much larger than a typical car radiator. The question is: How much larger and how much air friction must be overcome?

Effect of condenser size. - A first look at the answer is provided by figure 8. Condenser weight and fan power are plotted against condenser depth with frontal area as a parameter. The curves represent a difficult situation - the ambient air temperature is 80° F (300 K) and the engine is producing 175 shaft horsepower (130 kW). The fan power rises very steeply as depth is reduced. To avoid extreme fan power, a depth of at least 6 inches (15 cm) and a frontal area of about 6 square feet (0.56 m^2) are required. Such a condenser would occupy $3\frac{1}{2}$ cubic feet (0.1 m^3) and weigh about 130 pounds (60 kg) (about five times as much as a conventional radiator). The weight could be reduced to 50 pounds (23 kg) if aluminum were used in place of conventional radiator materials. The dashed curves show how ram air pressure due to car motion reduces the fan power expenditure. For instance, at 70 miles per hour (113 km/hr) the fan power is halved (from 17 to 8 hp (12.7 to 6 kW)) for the condenser dimensions just mentioned. Ram air cooling is not always available though, since car speed is not necessarily high during periods of high-power operation (e.g., pulling a heavy load up a hill). For this reason, the remaining data will be presented without the ram air cooling effect included. Also,

the condenser dimensions just mentioned are taken to be baseline values since they represent a reasonable design tradeoff of size and fan power. Many additional details for this baseline condenser are given in table I.

Effect of wheel power and ambient temperature. - Both the wheel power demand and the ambient air temperature have a very pronounced effect on the fan power and, hence, the required shaft power also. This is shown in figure 9 for the baseline condenser. The supplementary abcissa at the top of the figure reflects the car-speed-against-wheel-power relation of figure 5 for steady speed on a level road. Under most operating conditions, the fan requires only a negligible amount of power. For instance, for steady motion on a level road the fan power is never greater than 1 horsepower (0.7 kW) for speeds up to 80 miles per hour (130 km/hr) and ambient air temperatures not exceeding 100° F (311 K). But under some relatively infrequent conditions, the fan power can soar to extreme values. For example, climbing a 10-percent grade at 72 miles per hour (116 km/hr) requires 124 horsepower (92 kW) at the wheels (from fig. 5). If the ambient air temperature is 100° F (311 K), this combination of high power level and hot day causes the fan power to rise to 25 horsepower (19 kW).

The point is that under most conditions fan power extraction is of no concern; but when high power is demanded on very hot days, the fan power requirement becomes a dominant factor. This means that the condenser must be sized much larger than would otherwise be needed in order to satisfactorily handle the high-power/hot-day situation.

Effect of condensation temperature. - One obvious way to lower the high fan power levels is to raise the condensing steam temperature. This increases the temperature difference between the air and the water and thus lowers the airflow rate (for constant heat-transfer rate). Lower airflow rates have a very strong influence on the fan power requirement since air friction increases as some power between 2 and 3 of the airflow rate. Raising the condensation temperature lowers the thermodynamic efficiency of the basic steam cycle, however, so there is a tradeoff between fan power and thermal efficiency to be considered. Both fan power and overall powerplant efficiency are shown in figure 10 for the baseline condenser at full-power operation with ambient air temperature as a parameter. Note that at low condensation temperatures the overall efficiency drops sharply in response to the rapid rise in fan power, particularly for high ambient temperatures. The overall efficiency also diminishes at high condensation temperatures, but this reduction is due to a decrease in thermal efficiency (see fig. 7). As a result, there exists a maximum overall powerplant efficiency for each ambient air temperature.

It could be concluded from figure 10 that the 212° F (373 K) baseline condensation temperature is too low and that it ought to be raised to about 250° F (394 K). On an 80° F (300 K) day, for instance, the fan power is shown to decrease from 17 to 8 horsepower (13 to 6 kW) if the condensation temperature is raised from 212° to 250° F (373 to 394 K). Since this is accompanied by practically no change in the overall effi-

ciency, the 250° F (373 K) condensation temperature would appear to be the better choice. If the powerplant were always operated near its maximum power level on hot days, this would indeed be true; but at the typical off-design power levels usually experienced in automobiles, the curves of figure 10 would change shape and alter the above comparison. Under such typical conditions the overall efficiency would drop 7 percent (fig. 5) if the condensation temperature were raised from 212° to 250° F (373 to 394 K). The question then becomes one of comparing a 7 percent decrease in average efficiency with a 50 percent reduction in fan power under extremely difficult conditions. The answer to this question really involves other aspects as well (such as condensation pressure) and cannot be answered with definiteness here. Perhaps a temperature in between these two would be best in an overall sense.

In any case, it is apparent that full-power operation at air temperatures above 80° F (300 K) involves excessive fan power. Instead of constructing larger condensers to handle this situation, the curves of figure 10 suggest that it would be desirable to operate the powerplant not at a single condensation temperature but over a range of values whenever the fan power becomes excessive. The dashed lines on this figure show such an operating mode. Whenever the fan power demand exceeds the design limit (17 hp (13 kW) in this case), the condensation temperature is increased so as to keep the fan power from rising further. This mode of operation would permit high average efficiency with reasonable size condensers and fan mechanisms.

Boilers

In contrast with the condenser, the air-friction power of the boiler is independent of the ambient air temperature. The condenser airflow depends on the air temperature rise, which is limited by the steam condensation temperature. Thus, the condenser airflow must increase as the ambient air temperature rises in order to maintain a fixed power level. And this increases the air-friction power. But the boiler inlet air temperature is not a function of ambient air temperature - it is regulated by the burner controls. Therefore, changes in ambient air temperature do not alter the boiler airflow nor the air-friction power.

Of course, the power that the blower consumes is still strongly dependent on the power level (i. e., heat-transfer rate) of the boiler in the same fashion as for the condenser. For this reason, only the maximum blower power will be presented. This is at a full-power condition of 175 shaft horsepower (130 kW). As with the condenser, a baseline design is chosen for the boiler against which other designs are compared. The details of this baseline boiler are given in table II. Values of the six independent variables for the baseline boiler are (1) boiler outside diameter, 1.1 feet (0.335 m);

(2) boiler tube outside diameter, 0.5 inch (1.3 cm); (3) combustion gas inlet temperature, 3000° F (1920 K); (4) combustion gas outlet temperature, 300° F (420 K); (5) longitudinal tube pitch, 1.0; and (6) transverse tube pitch, 1.4. These are ranked in the order of the discussion that follows - which is the order of relative influence on boiler weight and blower power. These are the two primary criteria by which the various designs are judged; but there are others, such as boiler length, that are also important. Where it is appropriate, these other criteria are plotted in addition to weight and blower power.

Effect of boiler diameter and tube diameter. - Figure 11 shows the effect of outside boiler diameter on weight, blower power, boiler length, and maximum water pressure in the boiler tubes. Curves are given for four values of outside tube diameter. Increasing the boiler diameter causes the airflow per unit free-flow area to decrease. This results in a heat-transfer-coefficient reduction that, in turn, causes the heat-transfer area - and, hence, boiler weight - to increase. However, if the boiler diameter is reduced too far in an effort to save weight, the blower power rises sharply and the boiler length may also become limiting. A reasonable compromise occurs at the baseline diameter of 1.1 feet (0.335 m), where for 0.5-inch (1.3-cm) tubing the boiler weight is 97 pounds (44 kg), the blower power is 2.4 horsepower (1.8 kW), and the boiler length is 1.68 feet (0.513 m).

The tube diameter does not have a strong effect on blower power, but it does have a major influence on weight, length, and water pressure. As with boiler diameter, it is advantageous to use small-diameter tubing to reduce weight and boiler length up to a point. Decreasing the tube diameter much below 0.5 inch (1.3 cm) results in very large water-side pressure drops (inversely proportional to the fifth power of tube diameter). This causes the inlet water pressure (the maximum pressure) to increase rapidly; and this, in turn, increases the tube-wall thickness and boiler weight. The use of 0.4-inch (1-cm) tubing, for instance, has only a tiny weight advantage over 0.5-inch (1.3-cm) tubing and considerably higher maximum water pressure - 3400 instead of 2325 psia (23.5 instead of 16.0 MN/m^2) at the baseline point. This is an important consideration for the water pump design. Even the baseline value of 2325 psia (16 MN/m^2) is a difficult value to attain cheaply and reliably.

Effect of combustion gas inlet temperature. - Figure 12 shows the effect of changing the combustion gas inlet temperature. A low temperature is desirable from a materials standpoint and also to reduce air pollution. On the other hand, boiler weight and length and blower power all increase as the gas inlet temperature is reduced. This is due to the decreased average temperature difference between the gas and the water. The baseline value of 3000° F (1930 K) is below the temperature at which nitrogen oxides form readily, and considerably above the melting point of the modified 9M steel tube material. Should a dry tube condition develop without a rapid burner shutdown, the tube would, of

course, be destroyed. Therefore, a short-response-time temperature control would be needed to prevent tube burnout. If a more modest temperature were used, this problem would be alleviated at the expense of increased weight and blower power. At 2000° F (1370 K), the increase in weight would be 40 percent and the increase in blower power 400 percent. The maximum tube-wall temperature would decrease only slightly - from 1079° to 1045° F (855 to 836 K). This is so because the water-side heat-transfer coefficient is about 100 times higher than the gas-side coefficient.

Effect of combustion gas outlet temperature. - Picking the design value of combustion gas outlet temperature is a matter of trading overall efficiency for boiler weight, as shown in figure 13. The blower power is affected little. If the baseline outlet temperature were increased from 300° to 500° F (420 to 530 K), the boiler weight could be reduced from 97 to 63 pounds (44 to 29 kg), but the overall powerplant efficiency would drop from 0.186 to 0.174. This $6\frac{1}{2}$ percent drop in efficiency is not too serious, and it might be wise to raise the gas outlet temperature if more detailed studies reveal that the baseline boiler weight suggested here is unrealizable.

Effect of tube pitch. - The spacing of the tubes is governed by the longitudinal pitch x_l and transverse pitch x_t, as illustrated in sketch d. Close spacing is desirable from the standpoint of small boiler size and weight. Small size results mainly from the compact geometry of close spacing. Low weight and some size reduction is a result of relatively high gas velocity and, hence, high gas-side heat-transfer coefficients. But close spacing also results in high blower power and small separation spaces between neighboring tubes, as shown in figure 14. Small separation spaces are undesirable from the standpoint of fabrication difficulty with tight tolerances. This, in turn, leads to high cost. A single curve represents the separation space transverse to the gas flow, while separate curves are needed for the diagonal spacing.

The $x_l = 0.75$ curves (fig. 14) for weight and blower power are noticeably displaced from the other curves. This is caused by a combination of increased sensitivities, as x_l is reduced below 1.0, to gas flow rate per unit free-flow area and the gas-side friction factor. Values of x_l less than 1.0 call for a complicated three-dimensional tube bend in the connection between tube rows. Because of this, and the relatively high blower power and small diagonal spaces between tubes, values of x_l less than 1.0 are judged to be unattractive.

The baseline combination of $x_l = 1.0$ and $x_t = 1.4$ results in a good tradeoff between weight, blower power, and intertube separation. The diagonal intertube space of 0.11 inch (2.7 cm) could prove to be too small. If so, the best cure would be to increase x_l rather than x_t. For example, doubling the diagonal space by increasing x_l to 1.25 causes an 8 percent weight penalty and a 35 percent increase in boiler length (not shown in fig. 14). The blower power is barely affected. However, if the same spacing increase were achieved by raising x_t to slightly over 2.0, both the weight and

boiler length penalties are doubled. Partly offsetting this is a blower power reduction from 2.4 to 1.5 horsepower (1.8 to 1.1 kW). But since the blower power is small to begin with, this effect is not very significant. In any event, it is clear from this figure that 1.4 represents a minimum value of transverse tube pitch to avoid high blower power and 1.0 represents a lower limit on longitudinal pitch for the same reason plus those given above concerning fabrication problems.

Complete Propulsion System

Weight. - This section makes a somewhat rough comparison of steam and IC propulsion systems in terms of weight and fuel costs for a 4000-pound (1815-kg) passenger car. The weight comparison is given in table III, where the component weights are summed to determine the total propulsion system weight. It is only the total weight values that should be compared, not the individual component weights. Most of the component weights are not analyzed in this study but are taken from other reports on existing hardware. The IC-engine-powered-system data come from reference 18. No specific engine power is quoted in reference 18 for the average car but the steam-cars' power level provides at least average acceleration and top-speed performance. The Paxton steam powerplant (ref. 4) is linearly scaled-up (ref. 18) from 3350 to 4000 pounds (1380 to 1815 kg) gross car weight. It is rated at 143 shaft horsepower (107 kW) on a continuous basis and 179 shaft horsepower (133 kW) on a short-term basis. Since the pumps, fans, and other accessories are driven by an auxiliary turbine (powered by engine exhaust steam), nearly all this shaft power is available at the wheels. The Williams steam powerplant (ref. 1) is rated at 150 continuous shaft horsepower (112 kW) and 250 intermittent shaft horsepower (186 kW) and drives the accessories off the engine shaft.

The scaled-up Paxton steam powerplant is only 5 percent heavier than the IC powerplant, and the Williams steam powerplant is 6 percent heavier. It should be noted that the Williams powerplant as reported in reference 1 consists only of the engine (including pumps, controls, etc.) and the steam generator (including boiler, burner, blower, controls, and motor). The weight of the other essential items needed to complete the system are estimates by the present writer. In particular, the condenser weight is taken to be 130 pounds (59 kg) (from table I) plus another 30 pounds (14 kg) for the fan and drive mechanism.

Another comparison is shown in table III by the numbers in parentheses. This is for the same systems except that the boiler and condenser weights calculated in this study are used. The weight values are taken from tables I and II with allowances made for the fan and fan drive. The total steam-system weights are reduced by somewhat over 100 pounds, due mainly to decreased boiler weight. This causes the average

steam-system weight to drop to $2\frac{1}{2}$ percent less than the IC system. The steam-system weight could also be reduced another 80 pounds (36 kg) if aluminum were used for the condenser. Although this apparent steam-car advantage might be disclaimed on the grounds that the steam-system data do not yet represent a proven product suitable to the typical consumer, it does indicate that the propulsion system weight of such a steam car would probably not exceed the conventional IC-system weight by any substantial amount.

Fuel costs. - A tentative operating cost comparison can be made with the data in figure 15. Curves of fuel consumption against car speed are presented for three typical IC cars (ref. 19), the Paxton steam car (ref. 4), and a hypothetical steam car using the baseline data of tables I and II and figure 5. At off-design power, the engine expansion efficiency η_e of the hypothetical steam engine is assumed to decrease from its design value of 0.7 in the same ratio as that given for the Paxton powerplant (fig. 13 of ref. 4). Except for the 3335-pound (1380-kg) Paxton, all cars weigh very nearly 4000 pounds (1815 kg). The Paxton car can therefore be expected to be more economical than the hypothetical steam car, as is shown. The interesting point is that although the steam car appears slightly worse at high speeds it is better at low speeds, and thus the overall fuel consumption of the steam car can be expected to be essentially the same as that of the conventional IC car. Since steam-car fuels such as kerosene, diesel fuel, and low-octane gasoline are significantly cheaper than highly refined gasoline, the actual fuel cost is potentially less for the steam car. Steam-car fuel is certainly less expensive to produce. Whether the consumer would benefit if all cars were eventually steam powered is, of course, an open question; but at least the potential is there.

CONCLUDING REMARKS

The hypothetical boilers and condensers investigated were of conventional design for typical passenger cars. Present state-of-the-art materials and operating limits were observed for simplicity and to determine if, indeed, exotic designs or advances in the state of the art are necessary to produce a competitive steam powerplant. The results indicate that conventional designs should, in fact, be able to be synthesized into a steam powerplant comparable in weight and efficiency to today's IC powerplants. It is not obvious, on the other hand, that the steam powerplant offers any great advantage in weight or efficiency unless exotic designs prove otherwise. The advantage of steam lies in other aspects - mainly air pollution and noise.

The large baseline condenser would span the width of a car and require a pair of fans, side by side, instead of a single fan. Its large size is probably the most critical problem examined. Actually, it would seem that its weight disadvantage could be largely eliminated by using aluminum instead of brass and copper. This would reduce the weight

from 130 to 50 pounds (60 to 23 kg). Little hope is held for reducing the condenser size short of trading off powerplant efficiency or using variable condensation temperature operation. In any case, the baseline condenser, though relatively large, is certainly not a limiting component by itself.

The large condenser size is at odds with some existing steam-car condensers that are essentially just conventional automobile radiators. Apparently, these existing units were not designed with hot-day and high-power conditions in mind. They are adequate under normal conditions but either vent steam or demand excessive fan power under overload conditions.

Boilers, on the other hand, could apparently be made substantially smaller and lighter than they have in the past - perhaps by a factor of 2. This results mainly from using small-diameter tubing, small boiler diameter, and better materials. Large lengths of tubing are required, but this in itself is not too costly. For example, the 600 feet (180 m) of 0.5-inch (1.3-cm) tubing employed in the baseline boiler would cost $30.00 at the current price of $0.05 per foot ($0.16/m). If 316 stainless steel were used throughout, the weight would rise perhaps 30 percent and the price would more than double. It should also be pointed out that the assumed value of 2000 psia (13.8 MN/m^2) for the boiler outlet pressure is perhaps too high for this application. Lowering this pressure to 1500 psia (10.3 MN/m^2) or even lower would not seriously affect the overall efficiency but would certainly lessen the construction problems - particularly of the water pump, boiler tubing, and valves.

Additional research should be focused on (1) even more compact heat-exchanger designs, (2) exchangers using working fluids other than water, (3) stability and controls, (4) cost and practicality, and (5) overall system simulation. For example, different condenser and boiler configurations might produce significant size or weight reductions. Finned tubing might be advantageous in the liquid region of the boiler. Similarly, only water was assumed as a working fluid, although another fluid may in fact be superior in an overall sense. Apparently, nobody has really solved the water freezeup problem, and lubrication problems still exist despite many claims to the contrary. It is timely, therefore, to expend some effort in developing either a stable and cheap antifreeze and lubrication method, or a new working fluid tailored to the requirements of the Rankine automobile engine.

Nothing has been said here about potential two-phase stability problems. In fact, the whole problem of dynamics and controls should be the subject of future work. There is very little published information in these areas for steam-car systems.

Cost and practicality have barely been mentioned. Yet questions abound in these areas. For example, because of the large fan power consumption encountered during overloads, the fan drive mechanism is much more important than it is in present IC cars. The common belt-drive method would not suffice since the ratio of fan speed to

engine speed would vary depending on the driving conditions. Various fan drive methods should be investigated to determine the best system in terms of complexity, cost, weight, and controllability. Easy control is offered by electric motors, but they may be too large and expensive. Mechanical drives, on the other hand, might be too complicated and difficult to control. Perhaps a mechanical drive with a magnetic clutch would be best, but this is just a tentative suggestion.

Actually, a complete vehicle simulation is desirable in order to properly study the overall effects of the many variables involved. This should include the engine, the heat exchangers, the accessories, the body, the suspension system, the control system, a driving cycle, and so forth.

Lewis Research Center,
National Aeronautics and Space Administration,
Cleveland, Ohio, February 13, 1970,
126-15.

APPENDIX A

SYMBOLS

A	total heat-transfer area on one side of exchanger
A_c	minimum free-flow area on one side of exchanger
A_f	total fin area on one side of exchanger
A_{fr}	frontal area of heat exchanger
a/f	air-fuel ratio
B	condenser width
C_D	drag coefficient of car
C_f	correlation parameter for friction outside tube banks
C_{fr}	friction force coefficient for car
C_h	correlation parameter for heat transfer outside tube banks
C_p	specific heat at constant pressure
D	diameter of boiler
d	diameter of boiler tubing
F	force
F_G	flow configuration correction factor
f	flow Fanning friction factor
f/a	fuel-air ratio
G	mass flow rate per unit flow area
g	gravitational constant
H	specific enthalpy
h	heat-transfer coefficient
h_{fuel}	heating value of fuel
k	thermal conductivity
L_b	boiler length
L_c	condenser depth
L_{eq}	equivalent gas layer length
L_t	boiler tube length
l	effective fin length
M	molecular weight
m	$\sqrt{2h/kt}$
$\dot{m}$	mass flow rate
N_{coil}	number of coils per row of boiler tubing
N_{Pr}	Prandtl number, $\mu C_p/k$
N_R	Reynolds number, $4r_hG/\mu$
N_{row}	number of tube rows in boiler
N_{St}	Stanton number, h/GC_p
P	power
p	pressure
q	overall heat-transfer rate
R	universal gas constant
R_c	ratio of average circumference to inside circumference of condenser tubes
r_h	flow passage hydraulic radius

r_2, r_3	two-phase-flow friction factors
S	car frontal area
S_{allow}	allowable stress
T	temperature
t	thickness
U	overall thermal conductance
V_b	total volume of boiler
$V_{b,c}$	core volume of boiler
V_c	total volume of condenser
$V_{c,c}$	condenser core volume
V_{head}	condenser header volume
$\mathscr{V}$	car speed
v	specific volume
W	weight
X_d	density correction factor for humidity
x	percent of excess air in burner
x_l	ratio of longitudinal pitch to tube diameter
x_t	ratio of transverse pitch to tube diameter
Z	condenser core height
Z_{head}	condenser header height
α	heat-transfer area of one side of heat exchanger per unit total exchanger core volume
β	angle between road and horizontal
γ	specific-heat ratio
ϵ	emissivity
ξ	defined by eq. (B38)
η_b	boiler efficiency
η_{bl}	blower efficiency
η_e	engine expansion efficiency
η_f	fin temperature effectiveness
η_m	mechanical efficiency of engine
η_o	total surface-temperature effectiveness
η_{over}	overall powerplant efficiency
η_{pump}	water pump efficiency
η_{th}	thermal efficiency
μ	absolute viscosity
ρ	density
σ	free-flow area per unit frontal area, A_c/A_{fr}
σ^*	Stefan-Boltzmann constant
τ	fin pitch (number of fins per unit length)

Subscripts:

a	air
acc	accessories
aero	aerodynamic
b	boiler
bl	boiler blower
burn	burner
c	condenser
car	car

e	engine
f	condenser air-side fins
fan	condenser fan
fuel	fuel
g	gas-side of boiler
grav	gravity
head	condenser headers
i	inside
in	inlet
ℓ	liquid
ℓm	log-mean
m	mean value
max	maximum
min	minimum
o	outside
out	outlet
p	paint and dirt on air side
pump	water pump
r	radiation
s	superheat section
sat	saturation
sc	scale on water-side
sh	engine shaft
st	stoichiometric
t	tubes (boiler or condenser, as specified)
tire	tire
v	vapor
w	water
wall	wall
wh	car wheels
1	entrance
2	exit
3	condenser entrance
4	condenser exit

Superscripts:

$\bar{}$	average
'	ideal

APPENDIX B

BOILER CALCULATIONS

The details of the boiler calculations are set forth in this appendix, preceded by an outline of the general calculational scheme. Many of the symbols, equations, and data are taken directly from reference 15.

Outline of Calculation Scheme

The steps of the boiler calculations are as follows:

Step A - Assume values for the following independent parameters:

(1) Heat-transfer rate
(2) Tube outside diameter and tube material
(3) Tube spacing transverse and parallel to airflow
(4) Water temperatures at the condenser outlet and boiler outlet
(5) Combustion gas temperature at the boiler inlet and exhaust
(6) Steam outlet pressure
(7) Boiler diameter
(8) Blower efficiency

Step B - Estimate values for these dependent variables:

(1) Saturation water pressure in boiling region
(2) Tube-wall thickness in each region

Step C - Calculate

(1) Water properties at the inlet and outlet of each region
(2) Water-side enthalpy change in each region
(3) Airflow and airflow per unit free-flow frontal area
(4) Air temperatures at boiling-region inlet and outlet
(5) Air properties at the inlet and outlet of each region
(6) Air-side heat-transfer coefficients and friction factors at the inlet and outlet of each region

Step D - Calculate

(1) Inside tube diameter in superheat region
(2) Water-side heat-transfer coefficient at superheat-region outlet
(3) Superheat-region tube length and weight, based on outlet water-side and average (of inlet and outlet) air-side heat-transfer coefficients

(4) Maximum tube-wall temperature in superheat region
(5) New value of tube-wall thickness, based on inlet water pressure and maximum wall temperature
(6) Water-side pressure drop and inlet pressure for superheat region
(7) Iterate this entire step until inlet water pressure to the superheat-region converges

Step E - Repeat step D for the boiling region and then the liquid region, using the inlet water pressure of the preceding region as a first guess.

Step F - Compute the average water pressure in the boiling region. If this value does not agree with the estimated value of saturation pressure of step B, repeat steps C through E until the saturation pressure converges.

Step G - Sum the results of the three regions to determine the total boiler weight, volume, length, number of tube rows, and number of coils in each row.

Step H - Calculate the air-side pressure drop and the required blower power.

Details of Analysis

Geometry. - The details of this procedure constitute the remainder of this appendix. Some geometrical variables are calculated first. The gas-side net frontal area (see sketch b) is

$$A_{fr,g} = \frac{\pi}{4}\left(D_o^2 - D_i^2\right) \tag{B1}$$

where the boiler inside diameter D_i was assumed to be 0.3 times the outside diameter D_o. The minimum gas-side free-flow area $A_{c,g}$ may occur either transverse or diagonal to the gas flow. From the geometry in sketch d, the ratio of $A_{c,g}$ to $A_{fr,g}$ is

$$\left(\frac{A_c}{A_{fr}}\right)_g \equiv \sigma_g = \min\left\{\frac{x_t - 1}{x_t}, \frac{\sqrt{x_t^2 + 4x_l^2} - 2}{x_t}\right\} \tag{B2}$$

From the same sketch, the ratio of total gas-side heat-transfer area A_g to heat-exchanger core volume $V_{b,c}$ is

$$\frac{A_g}{V_{b,c}} \equiv \alpha_g = \frac{2\pi d_o}{2x_l d_o x_t d_o} = \frac{\pi}{x_l x_d d_o} \tag{B3}$$

If L_b denotes boiler length, the gas-side flow passage hydraulic radius $r_{h,g}$ is given by

$$r_{h,g} \equiv L_b\left(\frac{A_c}{A}\right)_g = \left(\frac{\sigma}{\alpha}\right)_g \tag{B4}$$

Water properties. - Both water properties (ref. 20) and steam properties (refs. 13 and 21) are readily determined from tables and equations once the temperatures and/or pressures are known. The steam outlet conditions are assumed parameters. The saturation pressure is at first taken to be the same as the steam outlet pressure and later refined when the pressure drops are calculated. The water entering the boiler comes from the condenser after passing through the water pump. Hence, the specific enthalpy of boiler inlet water is just

$$H_{w,in} = H_{w,c} + H_{pump} \tag{B5}$$

where H_{pump} is given by equation (3) and $H_{w,c}$ is determined from the assumed condensation temperature. The water-side enthalpy change in each region follows immediately since the enthalpy is now known at the inlet and outlet of each region.

Flow rates. - The water flow rate may then be found from equation (9). The gas flow follows from an energy balance:

$$\dot{m}_g = \dot{m}_w\left(\frac{\Delta H_w}{\Delta H_g}\right) \tag{B6}$$

The gas flow per unit free-flow frontal area is simply

$$G_g = \left(\frac{\dot{m}}{\sigma A_{fr}}\right)_g \tag{B7}$$

Air temperatures. - The gas temperature at the superheat-region outlet (same as boiling-region inlet) is determined from an energy balance:

$$\Delta H_{g,\,s} = \left(\frac{\dot{m}_w}{\dot{m}_g}\right)\Delta H_{w,\,s} \tag{B8}$$

where the subscript s denotes superheat region. Since all the right-side variables are known, the gas-side superheat enthalpy change $\Delta H_{g,\,s}$ is determined. Furthermore, the gas inlet temperature and enthalpy are known, so by subtraction of $\Delta H_{g,\,s}$ from the entrance enthalpy and use of appropriate temperature enthalpy tables, the gas temperature at the superheat outlet may be calculated. The gas temperature at the liquid-heating-region inlet (boiling-region outlet) is determined in a similar manner.

Air-side heat-transfer coefficients and friction factors. - All the inlet and outlet gas temperatures are now known, and the corresponding gas properties may be found by using tabular data (refs. 21 and 22). The gas-side Reynolds number is

$$N_{R,\,g} = \left(\frac{4r_h G}{\mu}\right)_g \tag{B9}$$

The local gas-side heat-transfer coefficients and Fanning friction factors may now be calculated from

$$h_g = \left(C_h C_p G N_{Pr}^{-2/3} N_R^{-0.4}\right)_g \qquad (300 < N_{R,\,g} < 15\,000) \tag{B10}$$

and

$$f_g = C_f N_{R,\,g}^{-0.18} \qquad (300 < N_{R,\,g} < 15\,000) \tag{B11}$$

where C_h and C_f are functions of x_ℓ and x_t as plotted in figures 33 and 34 of reference 15. The value of h_g at the superheat inlet is supplemented by a gas radiation term that is calculated with the equations and data of reference 21:

$$h_r = \frac{q_r}{T_g - T_w} = \frac{\left(q_r\right)_{CO_2} + \left(q_r\right)_{H_2O}}{T_g - T_w} \tag{B12}$$

$$\left(q_r\right)_{CO_2} = \sigma^* \epsilon_w \left(\epsilon_{CO_2} T_g^4 - \epsilon'_{CO_2} T_{wall}^4\right) \tag{B13}$$

$$\left(q_r\right)_{H_2O} = \sigma^* \epsilon_w \left(\epsilon_{H_2O} T_g^4 - \epsilon'_{H_2O} T_{wall}^4\right) \tag{B14}$$

Here σ^* is the Stefan-Boltzmann constant, ϵ_w is the tube-wall emissivity (assumed to be 0.8), ϵ_{CO_2} is the carbon dioxide emissivity at the gas temperature T_g, ϵ'_{CO_2} is the carbon dioxide emissivity at the tube-wall temperature T_{wall}, and similarly for the water vapor emissivities ϵ_{H_2O} and ϵ'_{H_2O}. The temperatures in equations (B13) and (B14) must be absolute temperatures. The carbon dioxide and water vapor emissivities are given in graphical form in reference 21 as a function of the product of equivalent gas layer length L_{eq} and partial pressures p_{CO_2} and p_{H_2O}:

$$L_{eq} = 3d_o(x_t - 1) \tag{B15}$$

$$p_{CO_2} = \frac{8}{52.75 + 58.5x} \tag{B16}$$

$$p_{H_2O} = \frac{8.5}{52.75 + 58.5x} \tag{B17}$$

$$x = \frac{(a/f) - (a/f)_{st}}{(a/f)_{st}} \tag{B18}$$

The partial pressure equations (B16) and (B17) apply to units of pressure in atmospheres. The stoichiometric air-fuel ratio $(a/f)_{st}$ is 14.9 (assuming the fuel to be C_8H_{17}). The air-fuel ratio a/f is related to the combustion gas temperature T_g by

$$a/f = \frac{h_{fuel}}{\left(H_g\right)_{T_g} - \left(H_g\right)_{in}} \tag{B19}$$

The tube-wall temperature T_{wall} in the radiation calculations is not known accurately (it is estimated to be 50° C above the steam exit temperature), but this is unimportant since the radiation heat transfer is very small compared to the convective heat transfer.

Water-side heat-transfer coefficient. - The water-side Reynolds number is calculated next by guessing the tube-wall thickness t_t:

$$N_{R,w} = \left(\frac{d_i G}{\mu}\right)_w \tag{B20}$$

where

$$d_i = d_o - 2t_t \tag{B21}$$

$$G_w = \frac{4}{\pi} \frac{\dot{m}_w}{d_i^2} \tag{B22}$$

The water-side heat-transfer-coefficient equation for coiled tubes is

$$h_w = \left\{ 0.023 \frac{k}{d_i} N_{Pr}^{0.4} N_R^{0.8} \left[N_R \left(\frac{d_i}{D_m} \right)^2 \right]^{0.05} \right\}_w \tag{B23}$$

The factor in brackets raised to the 0.05 power is due to coiled rather than straight tubing, according to reference 23. The mean coil diameter D_m is

$$D_m = D_o \sqrt{\frac{1}{2}\left[1 + \left(\frac{D_i}{D_o}\right)^2\right]} \tag{B24}$$

In the boiling region, h_w is multiplied by 3.6 to account for two-phase flow phenomena in accordance with graphical data in reference 24. Properties of the liquid phase are used for the boiling region.

Tube length and weight. - The average overall heat-transfer conductance for one particular region is

$$\frac{1}{U_g} = \frac{1}{\bar{h}_g} + \frac{1}{\left(\frac{d_i}{d_o}\right)_{h_w}} + \frac{2d_o t_t}{k_t(d_i + d_o)} \tag{B25}$$

The average gas-side heat-transfer coefficient $\bar{h}_g$ used in this equation is the arithmetic average of the inlet and outlet values of h_g multiplied by a correction factor given in figure 35 of reference 15 to account for a finite number of tube rows (i. e., the value of h_g given above is for an infinite number of tube rows). The number of tube rows is not yet known, however, so an estimate is made initially. A better estimate is calculated later and is used on the succeeding iteration. The value of h_w is taken to be the outlet value. This is not critical since h_w is of the order 50 $\bar{h}_g$ and d_i/d_o is slightly less than 1. The gas-side heat-transfer area of a region is calculated from the log-mean rate equation:

$$A_g = \frac{\dot{m}_g \Delta H_g}{U_g \Delta T_{lm}} \tag{B26}$$

where

$$\Delta T_{lm} \equiv \frac{\left(T_g - T_w\right)_{max} - \left(T_g - T_w\right)_{min}}{\ln\left[\frac{\left(T_g - T_w\right)_{max}}{\left(T_g - T_w\right)_{min}}\right]} \tag{B27}$$

For each region, the maximum temperature difference between the gas and water occurs at the gas-side inlet and the minimum difference occurs at the gas-side outlet. The tube length for each region is

$$L_t = \frac{A_g}{\pi d_o} \tag{B28}$$

and the tubing weight is

$$W_t = \pi \rho_t t_t (d_o - t_t) L_t \tag{B29}$$

Tube-wall temperature. - At this point it is necessary to check the tube-wall-thickness estimate made earlier. This requires knowing the maximum tube-wall temperature in each region. Sketch e illustrates the temperature profile through the tube

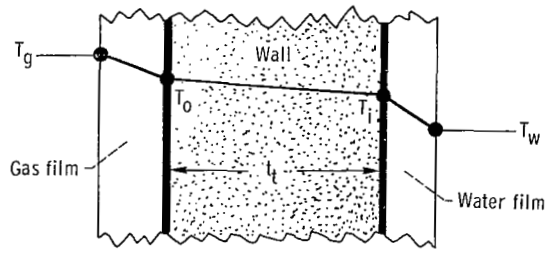

(e)

wall and fluid films. The tube-wall temperature may be determined from heat balance equations. Since for steady-state conditions the heat rate through the two fluid films equals the heat rate through the tube wall,

$$q = A_g h_g (T_g - T_o) = A_w h_w (T_i - T_w) = \frac{A_m k_t (T_o - T_i)}{t_t} \tag{B30}$$

But

$$A_g = \pi d_o L_t \tag{B31}$$

$$A_w = \pi d_i L_t \tag{B32}$$

$$A_m \equiv \frac{1}{2}(A_g + A_w) L_t = \frac{\pi}{2}(d_o + d_i) L_t \tag{B33}$$

$$d_i = d_o - 2t_t \tag{B21}$$

Substituting these four relations into the previous equation for q and rearranging yields

$$\frac{q}{\pi L_t d_o} = h_g (T_g - T_o) = \left(1 - \frac{2t_t}{d_o}\right) h_w (T_i - T_w) = \left(1 - \frac{t_t}{d_o}\right)\left(\frac{k}{t}\right)_t (T_o - T_i) \tag{B34}$$

(Gas film) (Water film) (Tube wall)

The gas-film and tube-wall parts of this expression may be used to solve for the inside wall temperature:

$$T_i = T_o - \frac{h_g(T_g - T_o)\left(\frac{t}{k}\right)_t}{1 - \frac{t_t}{d_o}} \tag{B35}$$

Likewise, the gas-film and water-film parts may also be used to solve for the inside wall temperature:

$$T_i = T_w + \frac{h_g}{h_w} \frac{T_g - T_o}{1 - \frac{2t_t}{d_o}} \tag{B36}$$

Finally, the last two expressions for T_i may be equated to solve for the outside tube-wall temperature:

$$T_o = \frac{T_w + \xi T_g}{1 + \xi} \tag{B37}$$

where

$$\xi \equiv \frac{\frac{h_g}{h_w}}{1 - \frac{2t_t}{d_o}} + \frac{\left(\frac{t}{k}\right)_t h_g}{1 - \frac{t_t}{d_o}} \tag{B38}$$

Tube-wall thickness. - A new estimate of tube-wall thickness may now be calculated using the thin-walled cylinder formula:

$$t_t = \frac{p_w d_o}{2S_{allow}} \tag{B39}$$

The allowable stress S_{allow} for modified 9M steel alloy is given in figure 2-44 of reference 16 as a function of temperature. Some representative values based on the outside wall temperature T_o are given in the following table:

Outside tube-wall temperature, T_o		Allowable stress, S_{allow}	
^oF	K	psia	MN/m^2
700	645	22 500	155.0
900	755	19 500	135.0
1100	865	10 400	71.5
1200	920	5 800	40.0

The pressure p_w in equation (B39) is initially taken to be the water outlet pressure to that particular region (e.g., 2000 psia (13.8 MN/m^2) in the superheat region). However, the pressure drop through the tube is substantial, and this implies that the water inlet pressure must be raised in order to hold the boiler outlet steam pressure constant. Furthermore, since the superheat region accounts for only about 10 percent of the total tube length, it consists of just the last two rows of tubing (typically). Thus, the geometry is such that the maximum superheat water pressure occurs at approximately the maximum wall temperature. Therefore, both the maximum water pressure and wall temperature were used to determine the tube-wall thickness even though both conditions do not occur at exactly the same point in each region.

Water-side pressure drop. - The water-side pressure drop was estimated with the equations contained in reference 25 for straight tubes modified by a correction factor for coiled tubes (ref. 23). Specifically,

$$\Delta p_w = \left[\frac{G^2(v_l - v_{l,sat})}{g} + \frac{fG^2(v_l + v_{l,sat})L_t}{d_i}\right]_w \quad \text{(liquid heating region)} \qquad \text{(B40)}$$

$$\Delta p_w = \left(\frac{v_l G^2}{g} r_2 + \frac{2fG^2 v_l L_t}{gd_i} r_3\right)_w \quad \text{(boiling region)} \qquad \text{(B41)}$$

$$\Delta p_w = \left[\frac{G^2(v_v - v_{v,sat})}{g} + \frac{fG^2(v_v + v_{v,sat})L_t}{gd_i}\right]_w \quad \text{(superheat region)} \qquad \text{(B42)}$$

where f_w is the Fanning friction factor for single-phase water flow in a coiled tube:

$$f_w = 0.046\, N_{R,w}^{-0.2}\left[N_{R,w}\left(\frac{d_i}{D_m}\right)^2\right]^{0.05} \tag{B43}$$

and r_2 and r_3 are two-phase flow factors dependent on pressure and steam quality that are plotted in figures 7 and 9 of reference 25. For $p_w = 2100$ psia (14.5 MN/m^2) and steam quality equal to 1.0, $r_2 = 5.664$ and $r_3 = 3.832$.

Iterations. - Replacing p_w with $p_w + \Delta p_w$ and using the new estimate of wall thickness, the step D calculations are repeated until convergence is obtained. The boiling-region calculations are done next using the p_w value just obtained for the superheat-region inlet. The tube-wall thickness for the boiling region is based on the maximum pressure and temperature in this region rather than being kept the same as for the superheat region. Similarly, the liquid-region calculations are done after those for the boiling region. Thus, there are three successive iterations, one for each region.

After the calculations for all three regions are completed, the assumed saturation pressure in the boiling region is checked using the average of the calculated inlet and outlet water pressure. If the two values do not agree, the step C through step E calculations are successively repeated until convergence is obtained. This is an iteration over the entire set of the three p_w iterations just discussed.

Boiler volume, length, and weight. - The total tube area, length, and weight are determined by summing the values of each region. The total boiler volume, including the central void, is

$$V_b = \frac{A_g}{\alpha_g\left[1 - \left(\frac{D_i}{D_o}\right)^2\right]} \tag{B44}$$

where A_g is the sum of the region areas. The boiler length is

$$L_b = \frac{4}{\pi}\frac{V_b}{D_o^2} \tag{B45}$$

and the number of tube rows (see sketch b) is

$$N_{row} = \frac{L_b}{x_l d_o} \tag{B46}$$

The number of coils per row is

$$N_{coil} = \frac{D_o\left(1 - \frac{D_i}{D_o}\right)}{2x_t d_o} \tag{B47}$$

The boiler weight is taken to be the total tube weight plus an allowance for the casing. The casing is assumed to consist of two 0.05-inch (0.13-cm) thick steel cylinders of diameter D_o. No weight estimate is included for the thermal insulation placed between the two casing walls, or for the controls, valves, or burner.

Gas-side pressure drop. - The gas-side pressure drop through the boiler core is calculated in each region with equation (24b) of reference 15.

$$\left(\frac{\Delta p}{p_1}\right)_g = \frac{G_g^2}{2g}\left(\frac{v_1}{p_1}\right)_g\left[(1 + \sigma^2)\left(\frac{v_2}{v_1} - 1\right) + f\left(\frac{A}{A_c}\right)\left(\frac{v_m}{v_1}\right)_g\right] \tag{B48}$$

Here f is the average Fanning friction factor and v_m is the mean specific volume. Subscripts 1 and 2 denote gas-side inlet and outlet, respectively. The mean specific volume is

$$v_m = \frac{1}{2}(v_1 + v_2) \qquad \text{(liquid and superheat regions)} \tag{B49}$$

$$v_m = \left(\frac{p_1}{\bar{p}}\right)\left(\frac{T_{lm}}{T_1}\right)v_1 \qquad \text{(boiling region)} \tag{B50}$$

where

$$\bar{p} = \frac{1}{2}(p_1 + p_2) \tag{B51}$$

$$p_2 = p_1 - \left(\frac{\Delta p}{p_i}\right)p_1 \tag{B52}$$

$$v_1 = \frac{1}{X_d}\left(\frac{RT_1}{Mp_1}\right) \tag{B53}$$

$$v_2 = \frac{1}{X_d}\left(\frac{RT_2}{Mp_2}\right) \tag{B54}$$

and,

$$T_{lm} = T_o + \frac{(T_{g,\,in} - T_o) - (T_{g,\,out} - T_o)}{ln\left(\frac{T_{g,\,in} - T_o}{T_{g,\,out} - T_o}\right)} \tag{B55}$$

There are two different equations (ref. 15) for v_m because the tube-wall temperature T_o is essentially constant in the boiling region but varies approximately linearly in the liquid and superheat regions. The density correction factor X_d for humidity and combustion products is found from data in reference 15 by assuming the ratio of water vapor to dry air is 0.015 and the ratio of hydrogen to carbon of the fuel to be 0.18. Initially, p_2 is estimated and then checked after the pressure drop is calculated. If the estimated value of p_2 does not agree with the calculated value, the pressure drop is recalculated with the new value of p_2. Two or three iterations usually produce an accuracy of 0.1 percent.

Blower power. - The boiler blower power is determined from the total gas-side pressure drop through an energy balance across the blower,

$$P_{bl} = \dot{m}_a \Delta H_a = \frac{\dot{m}_a C_p (\Delta T_a)'}{\eta_{bl}} = \frac{\dot{m}_a C_p T_1 \left[\left(1 + \frac{\Delta p}{p_1}\right)^{(\gamma-1)/\gamma} - 1\right]}{\eta_{bl}} \tag{B56}$$

The pressure drop is taken to be the sum of the three regional pressure drops (the burner pressure drop is neglected) and the blower efficiency η_{bl} is assumed to be 0.70.

Boiler Efficiency

Sketch f illustrates the fluid power network within the boiler-burner assembly.

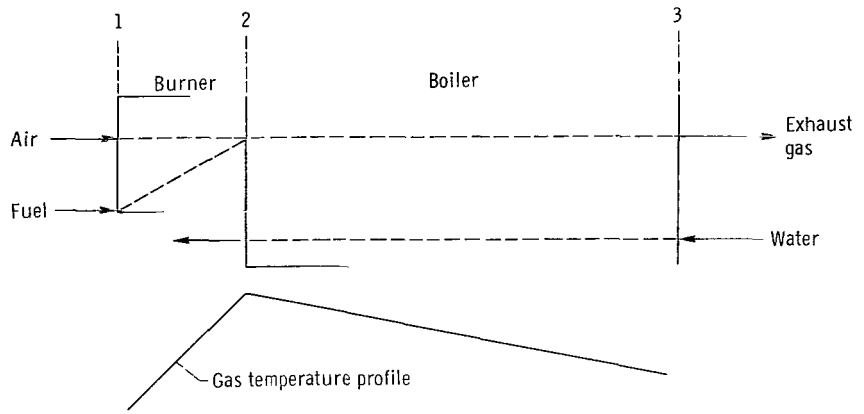

(f)

Assuming that the exhaust gas is air, the conservation of energy law states that

(Heat energy delivered by fuel) = (Increase in air energy) + (Increase in water energy)

or

$$\dot{m}_a(f/a)h_{fuel} = \dot{m}_a \Delta H_a + \dot{m}_w \Delta H_w \tag{B57}$$

where the combustion efficiency is assumed to be 100 percent. The boiler efficiency is defined as

$$\eta_b \equiv \frac{\text{Increase in water energy}}{\text{Heat energy delivered by fuel}} = \frac{\dot{m}_w \Delta H_w}{\dot{m}_a(f/a)h_{fuel}} \tag{B58}$$

Using equation (B57) to eliminate $(\dot{m}_w/\dot{m}_a)\Delta H_w$ yields

$$\eta_b = 1 - \frac{\Delta H_a}{(f/a)h_{fuel}} = 1 - \frac{\left(H_3 - H_1\right)_a}{(f/a)h_{fuel}} \tag{B59}$$

The subscripts on the air-side enthalpy are defined in sketch f. Also, considering the conservation of energy for the burner alone,

$$\dot{m}_a(f/a)h_{fuel} = \dot{m}_a\left(H_2 - H_1\right)_a \tag{B60}$$

and using this equation to eliminate $(f/a)h_{fuel}$ in equation (B59) yields

$$\eta_b = 1 - \left(\frac{H_3 - H_1}{H_2 - H_1}\right)_a \tag{B61}$$

The boiler efficiency is tabulated as follows for 80° F (300 K) ambient air temperature:

Maximum gas temperature in boiler, T_2		Exhaust gas temperature, T_3, °F (K)			
		200 (367)	300 (422)	400 (478)	500 (533)
		Boiler efficiency, η_b			
°F	K				
1500	1090	0.921	0.855	0.788	0.720
2000	1370	.943	.895	.847	.798
2500	1645	.956	.918	.881	.843
3000	1920	.964	.933	.903	.872

The gas tables of reference 22 were used to evaluate H_1, H_2, and H_3 as functions of the ambient, maximum, and exhaust gas temperatures, respectively..

APPENDIX C

CONDENSER CALCULATIONS

Many of the equations and data of reference 15 are used in the condenser analysis.

Volume and Weight

The total condenser volume V_c is the sum of the core volume $V_{c,c}$ and the header volume V_{head}. With the dimensions specified in the sketch g,

$$V_c = V_{c,c} + V_{head} = BZL_c + 2BZ_{head}L_c \tag{C1}$$

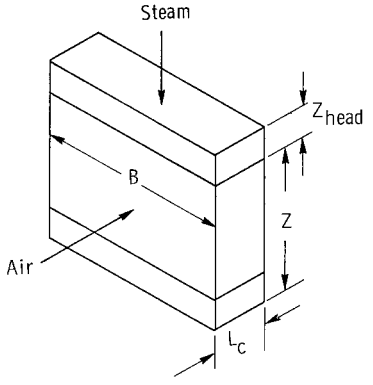

(g)

The condenser weight is

$$W_c = W_f + W_t + W_{head} \tag{C2}$$

where

$$W_f \cong (1 - \sigma_w)\rho_f t_f \tau V_{c,c} \tag{C3}$$

$$W_t = \rho_t t_t R_c \alpha_w V_{c,c} \tag{C4}$$

$$W_{head} = \rho_{head} t_{head} (2BL + 4BZ_{head} + 4L_c Z_{head}) \tag{C5}$$

Heat Transfer

In this study, the condenser configuration is specified and the independent variables are chosen to be the saturation temperature, the ambient air temperature, and the steam flow rate, as shown in sketch h.

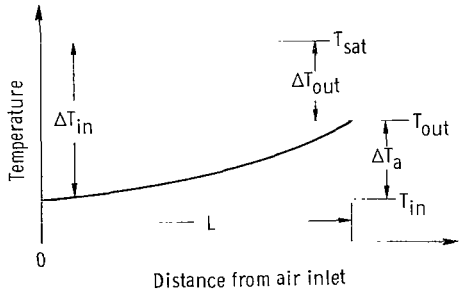

(h)

The primary dependent variable is the fan power required to overcome the air-side pressure drop. The calculations may be performed as follows: Assume the air-side outlet temperature to be T_{sat} - 25° F (270 K). Calculate the log-mean temperature:

$$\Delta T_{lm} = \frac{\Delta T_a}{\ln\left(\frac{\Delta T_{in}}{\Delta T_{out}}\right)} \tag{C6}$$

$$T_{lm} = T_{sat} - \Delta T_{lm} \tag{C7}$$

Determine air property data at T_{lm} using curve-fitted data from reference 21. These consist of the specific heat C_p, the viscosity μ_a, the thermal conductivity k_a, the Prandtl number N_{Pr}, and the specific volume v.

Calculate the airflow rate per unit area:

$$\dot{m}_a = \frac{\dot{m}_w \Delta H_w}{C_p \Delta T_a} \tag{C8}$$

$$G_a = \frac{\dot{m}_a}{ZB\sigma_a} \tag{C9}$$

Calculate the air-side Reynolds number:

$$N_{R,a} = \left(\frac{4r_h G}{\mu}\right)_a \tag{C10}$$

Using curve-fitted data of table 23 from reference 15, determine the basic heat-transfer parameter and the friction factor:

$$\left(N_{St} N_{Pr}^{2/3}\right)_a = \text{function of } N_{R,a}$$

$$f_a = \text{function of } N_{R,a} \tag{C11}$$

The air-side heat-transfer coefficient follows immediately from the definition of Stanton number:

$$h_a = \left[\frac{\left(N_{St} N_{Pr}^{2/3}\right)}{N_{Pr}^{2/3}} C_p G\right]_a \tag{C12}$$

The fin temperature effectiveness is calculated next:

$$\eta_f = \frac{\tanh m\ell}{m\ell} \tag{C13}$$

$$m \equiv \sqrt{\frac{2h_a}{k_f t_f}} \tag{C14}$$

Then the total surface-temperature effectiveness is

$$\eta_o = 1 - \left(\frac{A_f}{A}\right)_a (1 - \eta_f) \tag{C15}$$

The water-side flow rate per unit area is

$$G_w = \frac{\dot{m}_w}{BL_c\sigma_w} \tag{C16}$$

from which the water-side Reynolds number may be found

$$N_{R,w} = \left(\frac{4r_h G}{\mu}\right)_w \tag{C17}$$

The water-side heat-transfer coefficient is calculated from equation (13-4) of reference 26 for laminar condensate films:

$$h_w = 1.47\left(\frac{\mu_w}{k_w^3 \rho_w^2 g}\right)^{-1/3} \left(N_{R,w}\right)^{-1/3} \times 1.28 \tag{C18}$$

where the factor 1.28 is appended as recommended in reference 26.

Calculate the overall conductance per unit air-side area:

$$\frac{1}{U_a} = \frac{1}{\eta_o h_a} + \frac{1}{\left(\frac{\alpha_w}{\alpha_a}\right)h_w} + \frac{1}{\left(\frac{\alpha_w}{\alpha_a}\right)h_{sc}} + \frac{t_t}{\left(\frac{\alpha_w}{\alpha_a}\right)k_t} + \frac{t_t}{k_p} \tag{C19}$$

where the water-side scale deposit coefficient h_{sc} is assumed to be 500 Btu per hour per square foot per ^{o}F (2830 $W/(m^2)(K)$), the air-side paint and dirt thickness t_p is assumed to be 0.001 inch (0.0025 cm), and the conductivity k_p is assumed to be 0.75 Btu per hour per square foot per ^{o}F per foot (130 $W/(m)(K)$) (ref. 27).

Calculate a new air outlet temperature from the basic heat-transfer equation as follows:

$$q = U_a A_a \Delta T_{lm} \tag{C20}$$

Also,

$$q = \dot{m}_a C_p \Delta T_a \tag{C21}$$

Combining equations (C20) and (C21) yields

$$\Delta T_a = \frac{U_a A_a \Delta T_{lm}}{C_p \dot{m}_a} \tag{C22}$$

Now from the definition of ΔT_{lm} given in equation (C20),

$$T_{out} = T_{sat} - \Delta T_{out} = T_{sat} - \Delta T_{in} \exp\left(-\frac{\Delta T_a}{\Delta T_{lm}}\right) \tag{C23}$$

Substituting for ΔT_a gives

$$T_{out} = T_{sat} - \Delta T_{in} \exp\left(-\frac{\alpha_a V_c U_a}{C_p \dot{m}_a}\right) \tag{C24}$$

Where the relation $A_a = \alpha_a V_c$ has been used. This value of T_{out} is compared to the value assumed at the beginning of this procedure. If they do not closely agree, the entire procedure is repeated with the new value of T_{out}. Normally, three to six iterations are sufficient to produce an accuracy of 0.01 percent.

Air-side pressure drop and fan power. - The condenser air-side pressure drop and associated fan power are calculated with the same equations, (B48) and (B56), given in appendix B for the boiler. There is only one region instead of three, and equation (B50) is used to determine the mean specific volume. The wall temperature T_o is assumed to be the condensation temperature T_{sat}.

REFERENCES

1. Anon.: Automobile Steam Engine and Other External Combustion Engines. Joint Hearings before the Committee on Commerce and the Subcommittee on Air and Water Pollution of the Committee on Public Works, United States Senate, Serial No. 90-82, U.S. Government Printing Office, 1968.

2. Gouse, S. William, Jr.: Automotive Vehicle Propulsion. Part I: The Steam Engine and Part II: Total Energy Ecology Implications. Advances in Energy Conversion Engineering. ASME, 1967, pp. 917-926.

3. Gouse, S. W. Jr.: Steam Powered Automobile Should Come Back. Engineer, May-June 1968, pp. 22-26.

4. Dooley, J. L.; and Bell, A. F.: Description of a Modern Automotive Steam Powerplant. Paper S338, SAE, Jan. 1962.

5. Miner, S. S.: New Revolver-Like Steam Engine. Popular Sci., Feb. 1966, pp. 85-88.

6. Anon.: Air Pollution Fact Sheet. News Release, American Medical Assoc., Mar. 1966.

7. Morse, Richard S., Chairman: The Automobile and Air Pollution: A Program for Progress, Part I. Panel on Electrically Powered Vehicles, U.S. Department of Commerce, Oct. 1967.

8. Bjerklie, J. W.; and Sternlicht, B.: Critical Comparison of Low-Emission Otto and Rankine Engine for Automotive Use. Paper 690044, SAE, 1969.

9. Millman, V.: Advanced Technology Applied to the Steam Powered Vehicle. Paper 931A, SAE, 1964.

10. Ayres, Robert U.: Alternative Nonpolluting Power Sources. SAE J., vol. 76, no. 12, Dec. 1968, pp. 40-80.

11. Heffner, F. E.: Highlights From 6500 Hours of Stirling Engine Operation. SAE Trans., vol. 74, sect. 2, 1966, pp. 33-54.

12. Lienesch, John H.; and Wade, Wallace R.: Stirling Engine Progress Report: Smoke, Odor, Noise and Exhaust Emissions. Paper 680081, SAE, Jan. 1968.

13. Keenan, Joseph H.; and Keyes, Frederick G.: Thermodynamic Properties of Steam, Including Data for the Liquid and Solid Phases. John Wiley & Sons, Inc., 1936.

14. Kelly, K. B.; and Holcombe, H. J.: Aerodynamics for Body Engineers. Paper 649A, SAE, Jan. 1963.

15. Kays, W. M.; and London, A. L.: Compact Heat Exchangers. National Press, 1955.

16. Anon.: Selected Technology for the Electric Power Industry. NASA SP-5057, 1968.

17. Clark, Claude L.: Resumé of Investigations on Steels for High-Temperature, High-Pressure Applications, 1963-1965. Timken Roller Bearing Co., Steel and Tube Div., 1965.

18. Hoffman, G. A.: Systems Design of Electric Automobiles. Transportation Res., vol. 1, 1967, pp. 3-19.

19. Anon.: Five Full-Sized V8 Sedans. Consumers Reports, vol. 33, no. 1, Jan. 1968, pp. 24-33.

20. Jordan, W. B.: Fits to Thermodynamic Properties of Water. Rep. KAPL-M-6734, Knolls Atomic Power Laboratory, Nov. 1, 1967.

21. Eckert, E. R. G.; and Drake, Robert M., Jr.: Heat and Mass Transfer. Second ed., McGraw-Hill Book Co., Inc., 1959.

22. Keenan, Joseph H.; and Kayes, Joseph: Gas Tables. John Wiley & Sons, Inc., 1948.

23. Seban, R. A.; and McLaughlin, E. F.: Heat Transfer in Tube Coils with Laminar and Turbulent Flow. Int. J. Heat Mass Transfer, vol. 6, no. 5, May 1963, pp. 387-395.

24. Owhadi, Ali: Boiling in Self-Induced Radial Acceleration Fields. PhD Thesis, Oklahoma State Univ., 1966.

25. Thom, J. R. S.: Prediction of Pressure Drop During Forced Circulation Boiling of Water. Int. J. Heat Mass Transfer, vol. 7, no. 7, July 1964, pp. 709-724.

26. McAdams, William H.: Heat Transmission. Third ed., McGraw-Hill Book Co., Inc., 1954.

27. Marks, Lionel S., ed.: Mechanical Engineers' Handbook. Fifth ed., McGraw-Hill Book Co., Inc., 1951.

TABLE I. - DETAILS OF BASELINE CONDENSER

Overall dimensions:	
Width, B, ft; m	3; 0.915
Core height, Z, ft; m	2; 0.610
Header height (top and bottom), Z_{head}, in.; cm	2; 5.1
Depth, L_c, in.; cm	6; 15.2
Core volume, $V_{c,c}$, ft^3; m^3	3; 0.085
Total volume, V_c, ft^3; m^3	3.5; 0.099
Weight, lb; kg:	
Tubes (brass), W_t	57; 26
Fins (copper), W_f	66; 30
Headers (copper), W_{head}	7; 3
Total, W_c	130; 59
Air-side characteristics:	
Flow-passage hydraulic radius, $r_{h,a}$, ft; cm	0.00288; 0.0878
Heat-transfer area per unit core volume, α_a, ft^2/ft^3; m^2/m^3	270; 885
Ratio of minimum free-flow area to net frontal area, σ_a	0.780
Ratio of fin area to total area, $\left(A_f/A\right)_a$	0.845
Fin metal thickness, t_f, in.; cm	0.004; 0.01
Fin thermal conductivity, k_f, Btu/(hr)(ft)(^oF); W/(m)(K)	225; 399
Fin length, 1/2 distance between tubes, l, in.; cm	0.225; 0.57
Water-side characteristics (tubes have straight sides with semicircular ends):	
Outside tube dimensions, in.; cm	0.737 by 0.10; 1.87 by 0.254
Inside tube dimensions, in.; cm	0.717 by 0.08; 1.82 by 0.203
Flow-passage hydraulic radius, $r_{h,w}$, ft; cm	0.00306; 0.0943
Heat-transfer area per unit core volume, α_w, ft^2/ft^3; m^2/m^3	42.1; 138
Ratio of minimum free-flow area to net frontal area, σ_w	0.129
Tube metal thickness, t_t, in.; cm	0.01; 0.0254
Tube thermal conductivity, k_t, Btu/(hr)(ft^2)(^oF/ft), W/(m)(K)	60; 104
Header metal thickness, t_{head}, in.; cm	0.030; 0.0762
Condensation temperature, T_{sat}, ^oF; K	212; 373
Values for design conditions[a]:	
Air outlet temperature, T_{out}, ^oF; K	153; 341
Airflow, $\dot{m}_a$, lb/hr; kg/hr	80 200; 36 400
Airflow per unit free-flow area, G_a, lb/(hr)(ft^2); kg/(hr)(m^2)	17 033; 83 300
Air-side heat-transfer coefficient, h_a, Btu/(hr)(ft^2)(^oF); W/(m^2)(K)	30.7; 174
Air-side friction factor, f_a	0.0229
Air-side pressure drop, $\Delta p/p_1$	0.0103
Fan power, P_{fan}, hp; kW	17; 12.6
Water flow, $\dot{m}_w$, lb/hr; kg/hr	1463; 664
Water flow per unit free-flow area, G_w, lb/(hr)(ft^2); kg/(hr)(m^2)	7564; 37 000
Water-side heat-transfer coefficient, h_w, Btu/(hr)(ft^2)(^oF); W/(m^2)(K)	2043; 11 600
Heat-transfer rate, P_c, Btu/hr; W	1 425 000; 417 000

[a]175 shaft horsepower (130 kW) on 80° F (300 K) day.

TABLE II. - DETAILS OF BASELINE BOILER

Overall dimensions:	
Outside diameter, D_o, ft; m	1.1; 0.335
Length, L_b, ft; m	1.68; 0.513
Net frontal area, $A_{fr,g}$, ft^2; m^2	0.865; 0.0804
Total volume, V_b, ft^3; m^3	1.60; 0.045
Weight, lb; kg:	
Tubing (modified 9M steel alloy)	84.5; 38.4
Casing (steel)	12.5; 5.7
Total	97.0; 44.1
Tube geometry and temperature:	
Number of tube rows, N_{row}	40
Number of coils per row, N_{coil}	6
Longitudinal pitch, x_l	1.0
Transverse pitch, x_t	1.4
Minimum distance between tubes (occurs diagonal to gas flow), in.; cm	0.11; 0.28
Total heat-transfer area, A_g, ft^2; m^2	78; 7.25
Outside tube diameter, d_o, in.; cm	0.5; 1.27
Tube-wall thickness, t_t, in.; cm	
Superheat region	0.0485; 0.123
Boiling region	0.0243; 0.0617
Liquid region	0.0253; 0.0640
Tube length, L_t, ft; m	
Superheat region	49; 15
Boiling region	83; 25
Liquid region	468; 142
Maximum wall temperature, T_o, ^oF; K:	
Superheat region	1079; 855
Boiling region	661; 623
Liquid region	664; 625
Tube material thermal conductivity, k_t, Btu/(hr)(ft)(^oF); W/(m)(K)	16; 28.4

TABLE II. - Concluded. DETAILS OF BASELINE BOILER

Gas-side characteristics of design power[a]:	
Gas flow, $\dot{m}_g$, lb/hr; kg/hr	2546; 1158
Gas flow per unit net frontal area, G_g, lb/(hr)(ft^2); kg/(hr)(m^2)	10 300; 50 400
Ratio of minimum free-flow area to net frontal area, σ_g	0.286
Ratio of heat-transfer area to core volume, α_g	53.9
Flow-passage hydraulic radius, $r_{h,g}$, ft; m	0.0053; 0.00162
Boiler efficiency, η_b	0.933
Fanning friction factor, f_a (average)	0.0535
Pressure drop, $\left(\Delta p/p_1\right)_g$	0.0466
Blower power, P_{bl}, hp; kW	2.41; 1.80
Inlet temperature, $T_{g,in}$; ^{o}F; K:	
Superheat region	3000; 1920
Boiling region	2311; 1540
Liquid region	1438; 1055
Outlet temperature, liquid region, $T_{g,out}$, ^{o}F; K	300; 422
Average heat-transfer coefficient, h_g, Btu/(hr)(ft^2)(^{o}F); W/(m^2)(K):	
Superheat region	46.5; 263
Boiling region	50.0; 283
Liquid region	42.2; 239
Water-side characteristics at design power[a]:	
Water flow, $\dot{m}_w$, lb/hr; kg/hr	1482; 674
Superheat outlet pressure, $\left(p_{w,out}\right)_s$, psia; MN/m^2	2000; 13.8
Inlet pressure, $p_{w,in}$, psia; MN/m^2:	
Superheat region	2178; 15.0
Boiling region	2244; 15.5
Liquid region	2329; 16.0
Superheat outlet temperature, $T_{w,out}$, ^{o}F; K	1000; 810
Inlet temperature, $T_{w,in}$, ^{o}F; K:	
Superheat region	648; 615
Boiling region	652; 618
Liquid region	234; 386
Water inventory, lb; kg	26; 12
Heat-transfer rate, P_b, Btu/hr; W	1 900 000; 557 000
Ratio of water flow to shaft power, lb/hp-hr; kg/W-hr	8.47; 5.18

[a]175 shaft horsepower (130 kW).

TABLE III. - WEIGHT COMPARISON

OF AUTOMOBILE POWERPLANTS

[Car weight, 4000 lb; 1820 kg.]

Component	Weight	
	lb	kg
Conventional internal combustion powerplant[a]		
Engine[b]	600	272
Transmission	160	73
Starter	20	9
Rear axle, drive line	172	78
Exhaust, smog control	56	25
Battery	48	22
Generator, controls	20	9
Radiator (full)	56	25
Fuel tank (full)	176	80
Total	1308	593
Scaled-up Paxton steam powerplant[c, d]		
Engine[b]	490	222
Transfer case and differential	78	35
Steam generator[e]	267 (167)	121 (76)
Condenser, fan, drive	167 (160)	76 (73)
Exhaust turbine	18	8
Battery[f]	48	22
Generator, controls	24	11
Hotwell	24	11
Water, oil	72	33
Fuel tank (full)[f]	190	86
Total	1378 (1271)	625 (577)
Williams steam powerplant[g]		
Engine[b]	342	155
Clutch[f]	50	23
Steam generator[e]	276 (167)	125 (76)
Condenser, fan, drive[f]	160 (160)	72 (73)
Rear axle, drive line[f]	172	78
Battery[f]	48	22
Alternator, controls[f]	24	11
Hotwell[f]	24	11
Water, oil[f]	100	45
Fuel tank (full)[f]	190	86
Total	1386 (1277)	628 (580)

[a] From ref. 18.

[b] Includes pump, controls, wiring, piping, flues, and valves.

[c] From ref. 4 (data linearly scaled from 3350 lb (1380 kg) car weight).

[d] Values in parentheses are alternate values based on tables I and II.

[e] Includes boiler, burner, blower, motor, insulation, and controls.

[f] Not included in reference data, but estimated by present writer.

[g] From ref. 1.

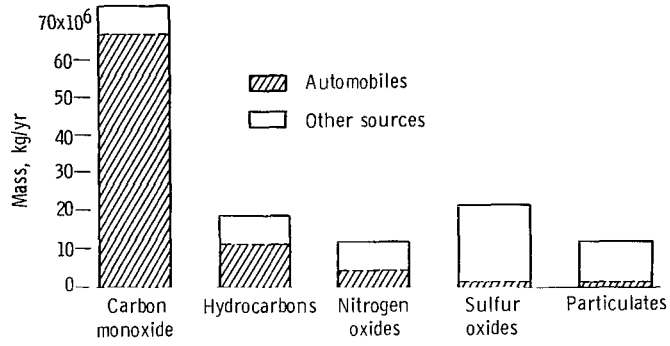

Figure 1. - Individual contaminants by source for 1966. (From ref. 7).

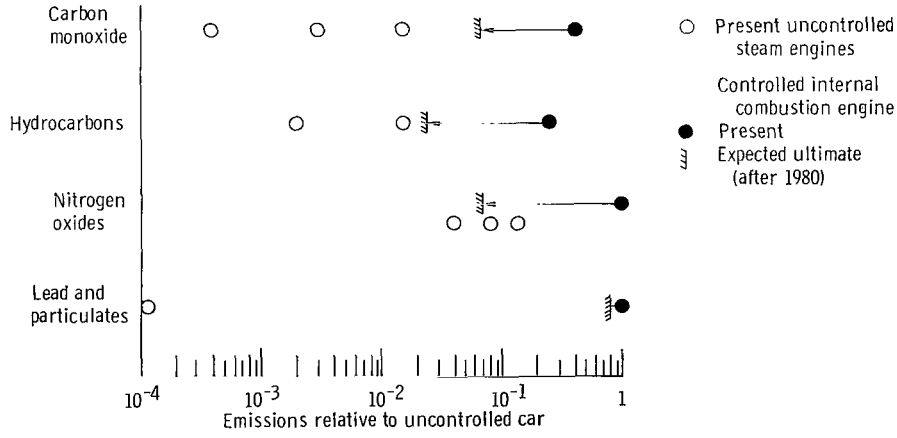

Figure 2. - Emission comparisons. (Data compiled from refs. 1 and 7.)

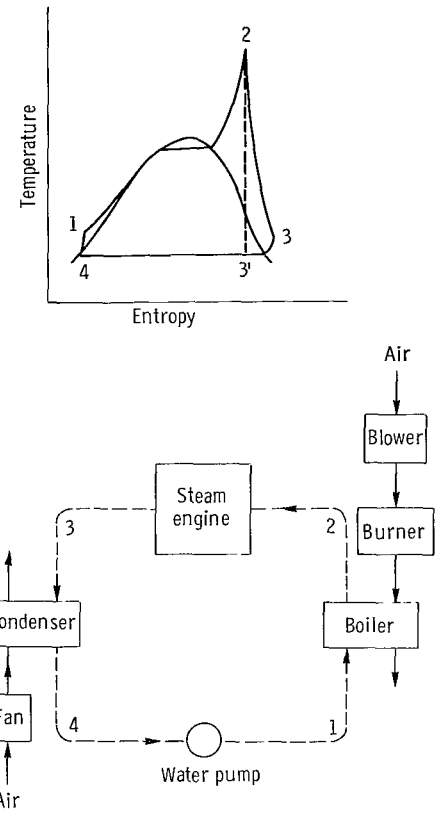

Figure 3. - Schematic diagram of simple steam cycle.

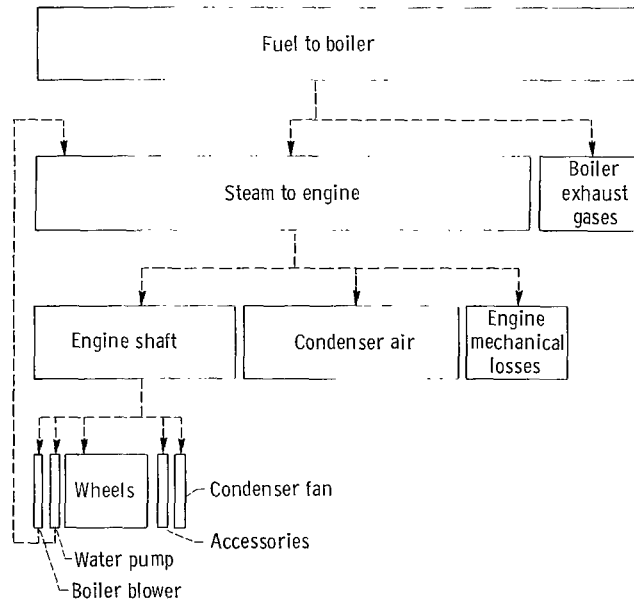

Figure 4. - Energy flow model for steam car.

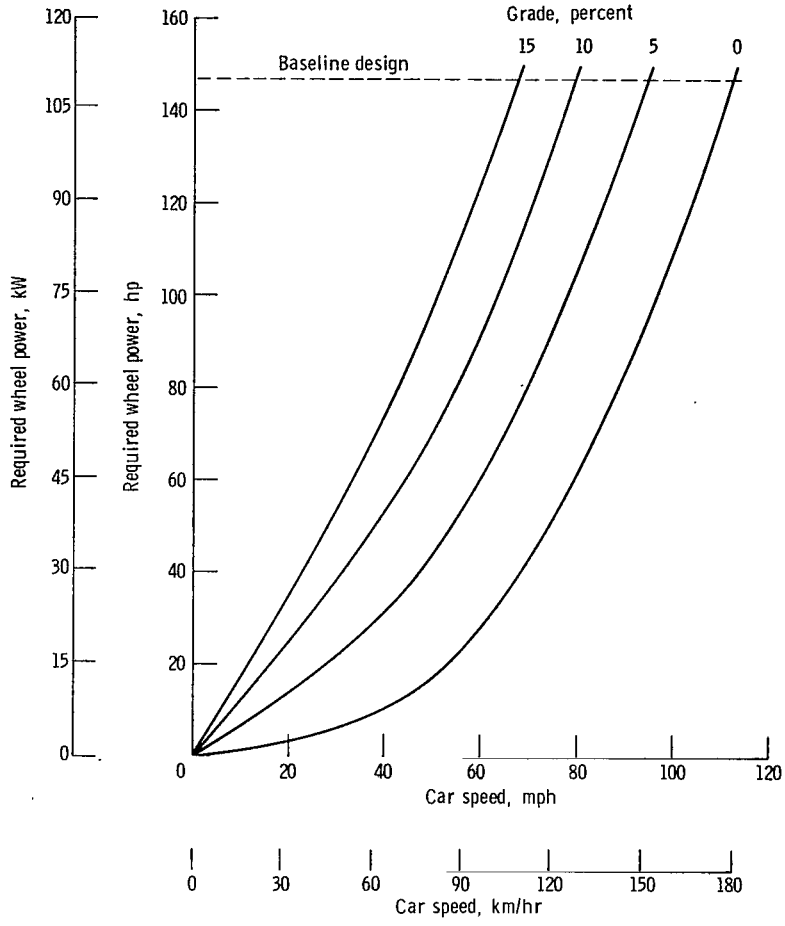

Figure 5. - Required wheel power for passenger car. Steady motion; no wind; car weight, 4000 pounds (1815 kg); frontal area, 24 square feet (2.23 m^2); drag coefficient, 0.45.

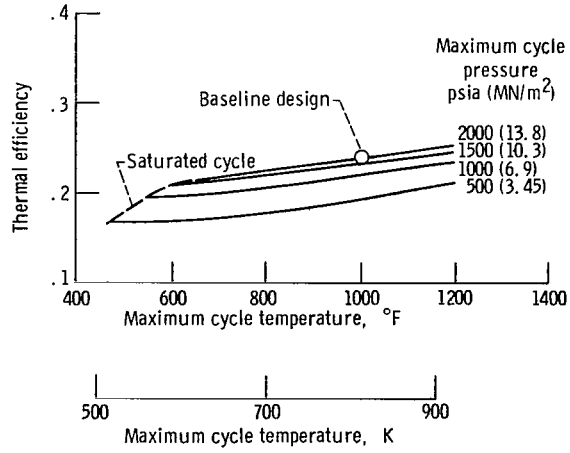

Figure 6. - Effect of maximum cycle temperature and pressure on thermal efficiency. Pump efficiency, 0.5; engine efficiency, 0.7; pressure drop neglected; condenser temperature, 212° F (373 K).

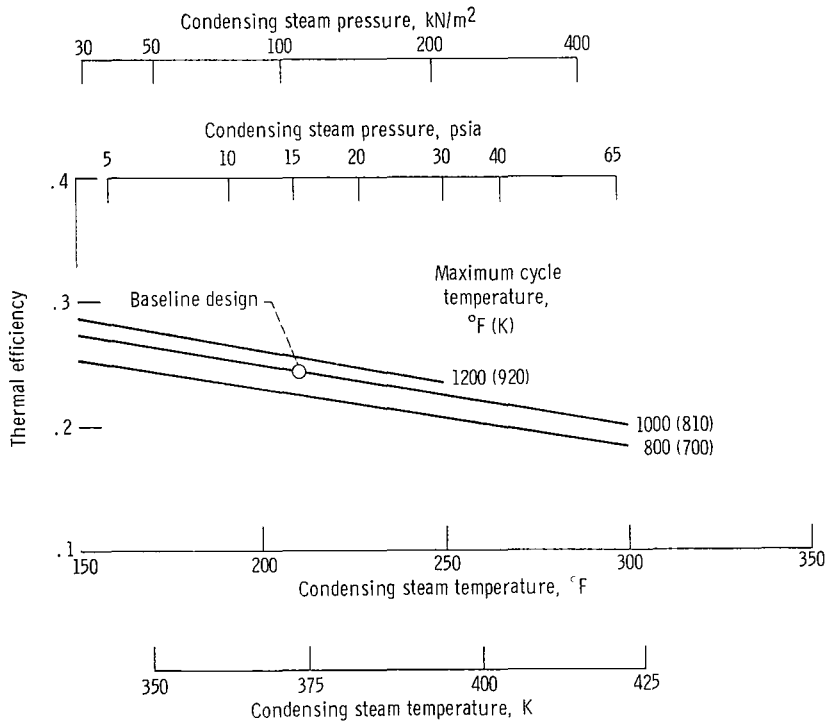

Figure 7. - Effect of condensing steam temperature on thermal efficiency. Pump efficiency, 0.5; engine efficiency, 0.7; pressure drop neglected; maximum cycle pressure, 2000 psia (13.8 MN/m2).

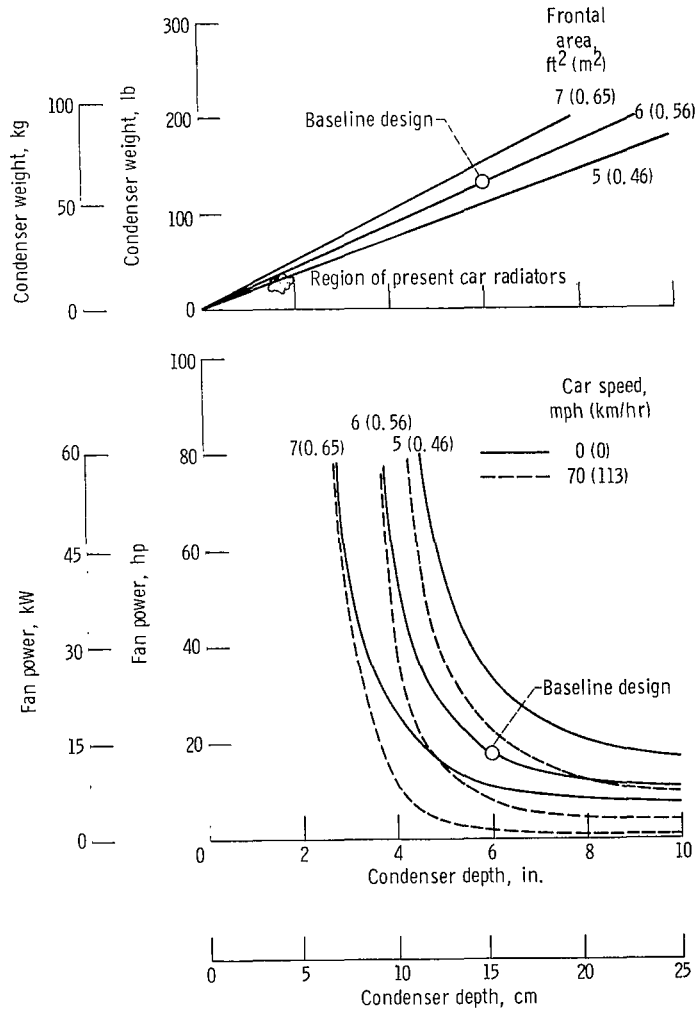

Figure 8. - Effect of condenser size on performance. Shaft power, 175 horsepower (130 kW); ambient temperature, 80° F (300 K); condensation temperature, 212° F (373 K); fan efficiency, 0.7; copper fins; brass tubes.

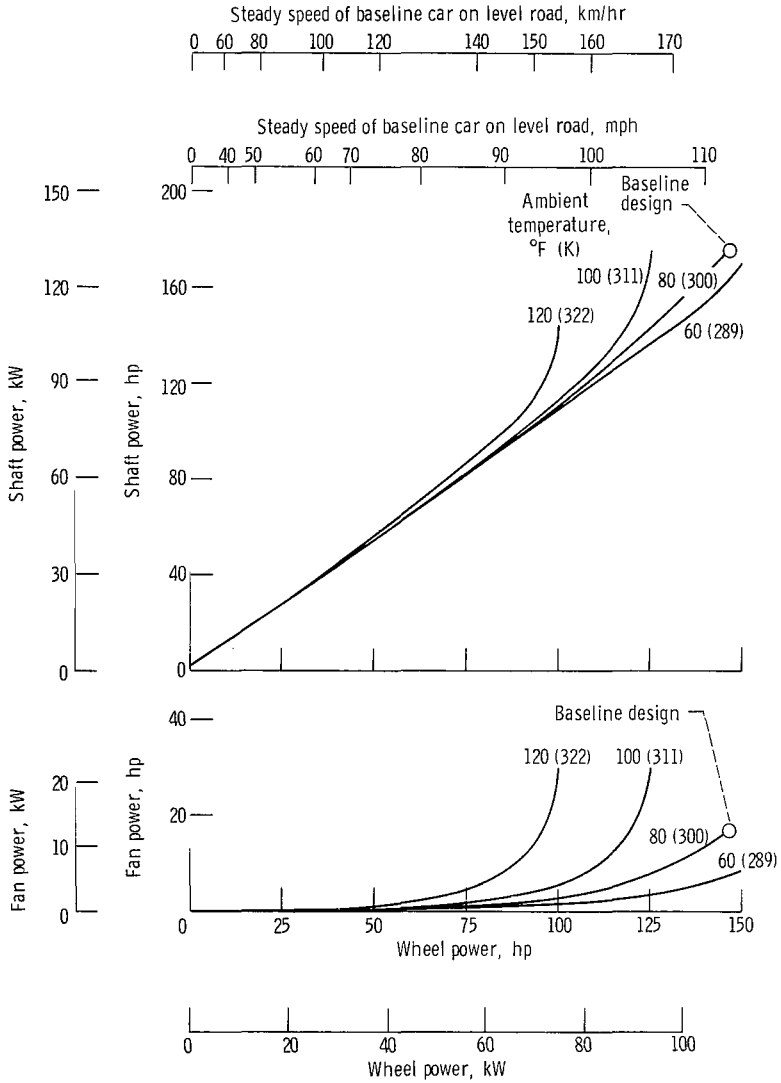

Figure 9. - Effect of wheel power and ambient temperature on fan and shaft power. Condenser frontal area, 6 square feet (0.56 m^2); condenser depth, 6 inches (15 cm); condensation temperature, 212° F (373 K); relative wind effect ignored.

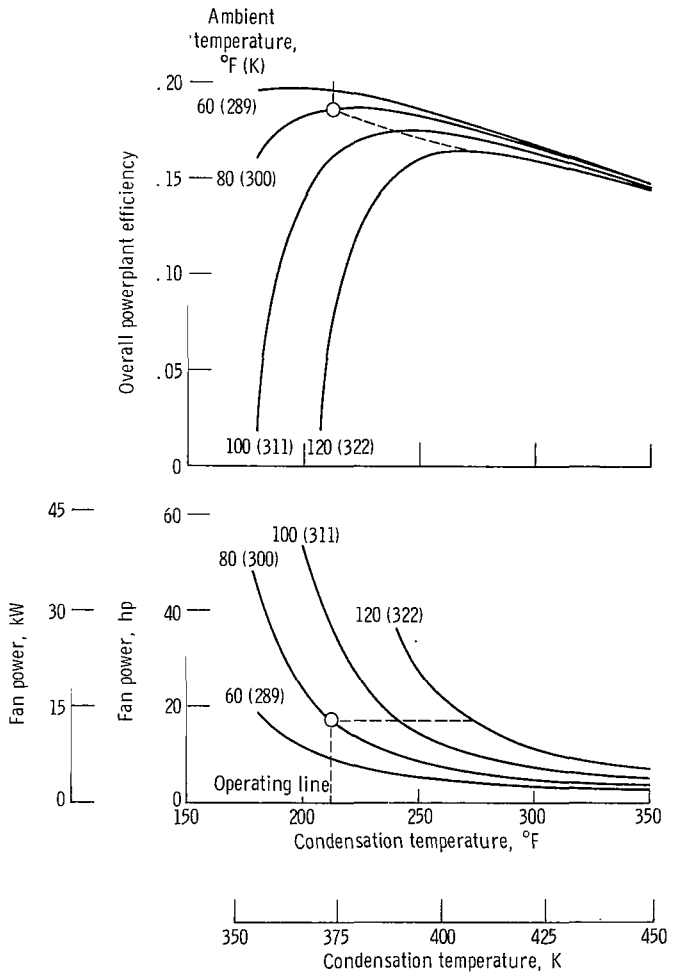

Figure 10. - Effect of condensation temperature on fan power and overall powerplant efficiency. Shaft power, 175 horsepower (130 kW); condenser frontal area, 6 square feet (0.56 m^2); condenser depth, 6 inches (15 cm); fan efficiency, 0.7; relative wind effect ignored.

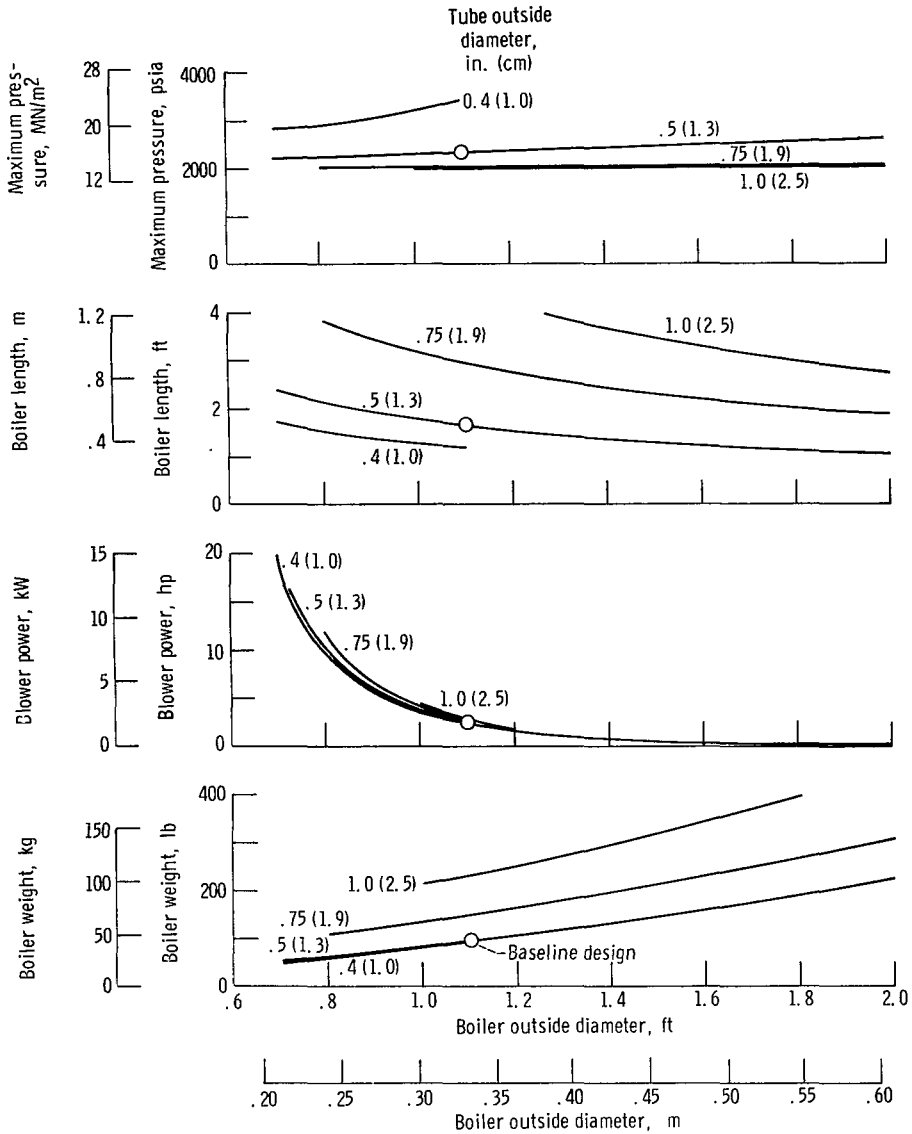

Figure 11. - Effect of boiler diameter and tube diameter on boiler weight, length, blower power, and maximum water pressure. Gas inlet temperature, 3000° F (1920 K); gas outlet temperature, 300° F (420 K); shaft power, 175 horsepower (130 kW); tube pitch; longitudinal, 1.0, and transverse, 1.4; tube material, modified 9M steel alloy; steam temperature, 1000° F (810 K); steam pressure, 2000 psia (13.8 MN/m²); blower efficiency, 0.7.

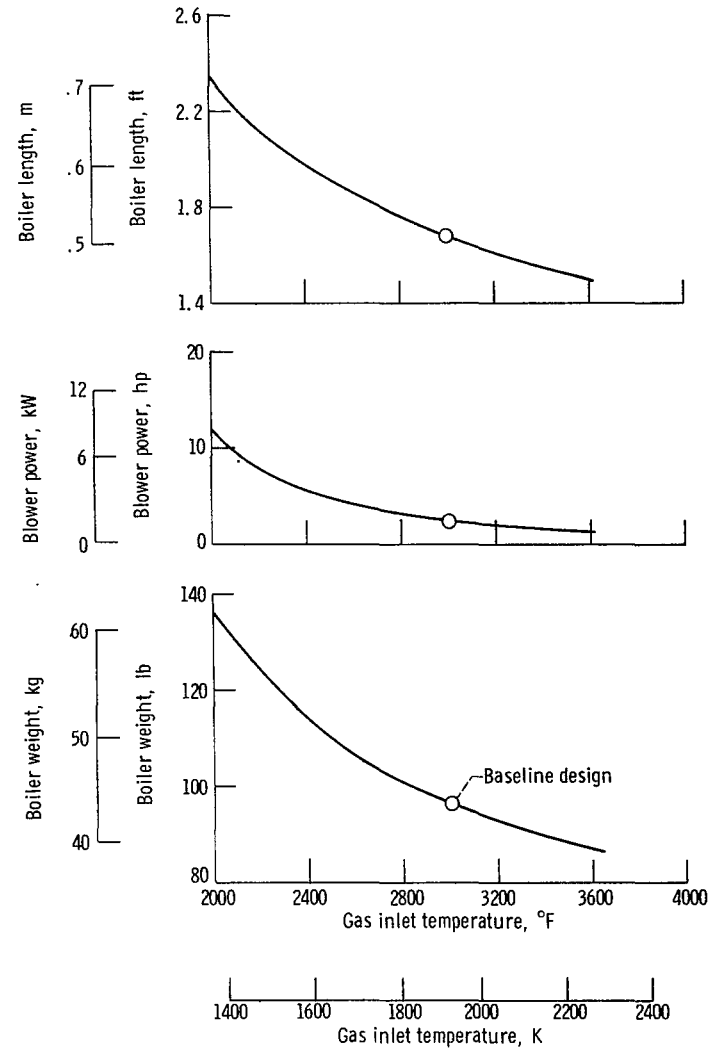

Figure 12. - Effect of combustion gas inlet temperature on boiler weight, length, and blower power. Boiler outside diameter, 1.1 feet (0.335 m); tube outside diameter, 0.5 inch (1.3 cm); gas outlet temperature, 300° F (420 K); shaft power, 175 horsepower (130 kW); tube pitch: longitudinal, 1.0, and transverse, 1.4; tube material, modified 9M steel alloy; steam temperature, 1000° F (810 K); steam pressure, 2000 psia (13.8 MN/m²); blower efficiency, 0.7.

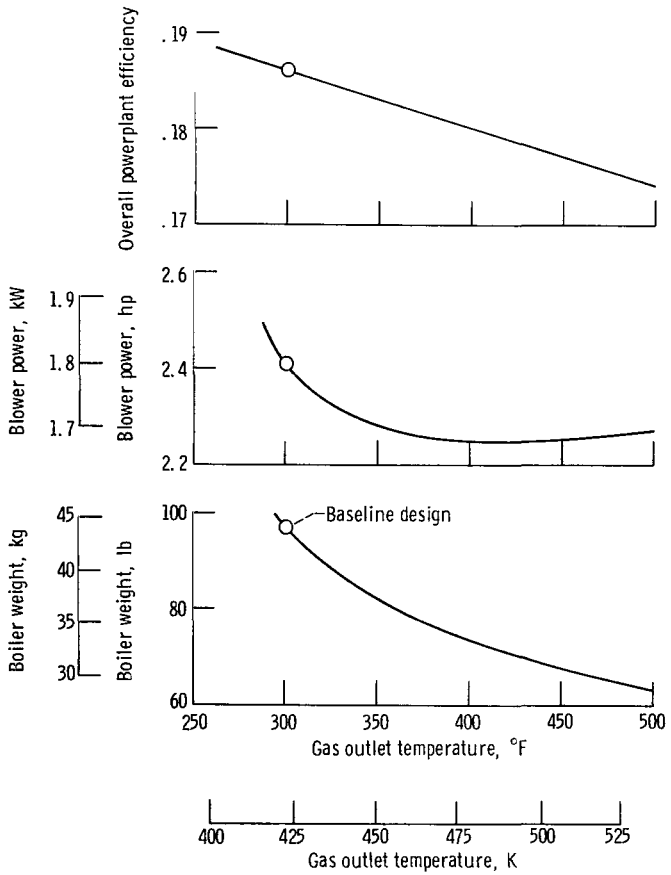

Figure 13. - Effect of gas outlet temperature on boiler weight, blower power, and overall powerplant efficiency. Boiler outside diameter, 1.1 feet (0.335 m); tube outside diameter, 0.5 inch (1.3 cm); gas inlet temperature, 3000° F (1930 K); shaft power, 175 horsepower (130 kW); tube pitch: longitudinal, 1.0, and transverse, 1.4; tube material, modified 9M steel alloy; steam temperature, 1000° F (810 K); steam pressure, 2000 psia (13.8 MN/m^2); blower efficiency, 0.7.

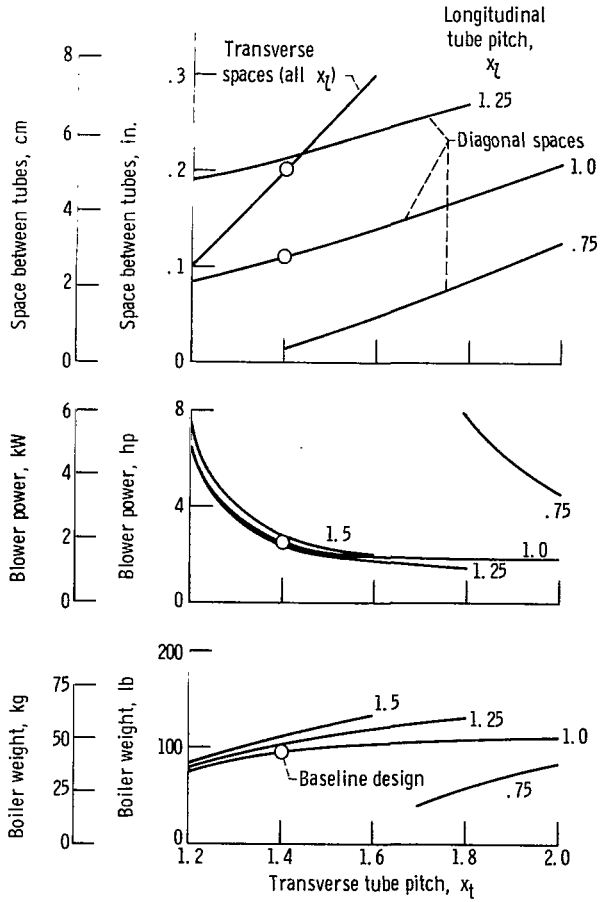

Figure 14. - Effect of tube pitch on boiler weight, blower power, and separation space between tubes. Boiler outside diameter, 1.1 feet (0.335 m); tube outside diameter, 0.5 inch (1.3 cm); gas inlet temperature, 3000° F (1930 K); gas outlet temperature, 300° F (420 K); shaft power, 175 horsepower (130 kW); tube material, modified 9M steel alloy; steam temperature, 1000° F (810 K); steam pressure, 2000 psia (13.8 MN/m^2); blower efficiency, 0.7.

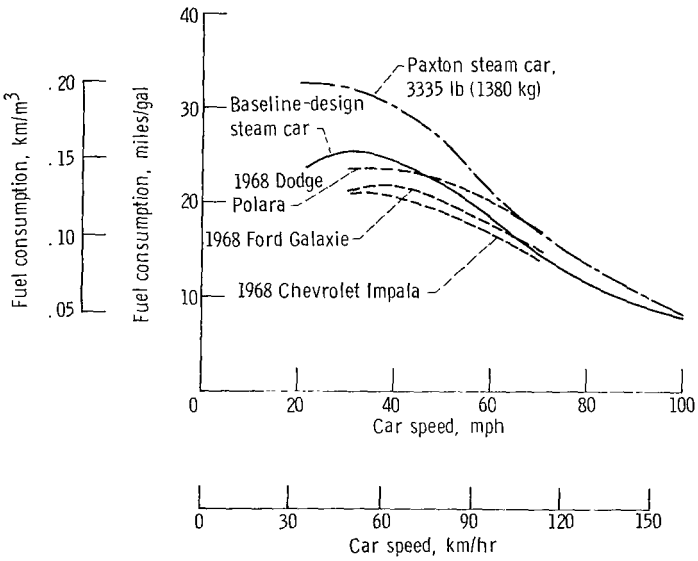

Figure 15. - Fuel economy comparison of baseline-design steam car and existing automobiles. Level, steady motion; no wind; car weight, 4000 pounds (1815 kg) except as noted.

NASA-Langley, 1970 —— 28 E-5275

"The aeronautical and space activities of the United States shall be conducted so as to contribute . . . to the expansion of human knowledge of phenomena in the atmosphere and space. The Administration shall provide for the widest practicable and appropriate dissemination of information concerning its activities and the results thereof."

—NATIONAL AERONAUTICS AND SPACE ACT OF 1958

NASA SCIENTIFIC AND TECHNICAL PUBLICATIONS

TECHNICAL REPORTS: Scientific and technical information considered important, complete, and a lasting contribution to existing knowledge.

TECHNICAL NOTES: Information less broad in scope but nevertheless of importance as a contribution to existing knowledge.

TECHNICAL MEMORANDUMS: Information receiving limited distribution because of preliminary data, security classification, or other reasons.

CONTRACTOR REPORTS: Scientific and technical information generated under a NASA contract or grant and considered an important contribution to existing knowledge.

TECHNICAL TRANSLATIONS: Information published in a foreign language considered to merit NASA distribution in English.

SPECIAL PUBLICATIONS: Information derived from or of value to NASA activities. Publications include conference proceedings, monographs, data compilations, handbooks, sourcebooks, and special bibliographies.

TECHNOLOGY UTILIZATION PUBLICATIONS: Information on technology used by NASA that may be of particular interest in commercial and other non-aerospace applications. Publications include Tech Briefs, Technology Utilization Reports and Notes, and Technology Surveys.

Details on the availability of these publications may be obtained from:

SCIENTIFIC AND TECHNICAL INFORMATION DIVISION

NATIONAL AERONAUTICS AND SPACE ADMINISTRATION

Washington, D.C. 20546